

# Repurposing ubiquitination for innovative antibody conjugation

Hebieshy, A.F. el

#### Citation

Hebieshy, A. F. el. (2025, October 16). *Repurposing ubiquitination for innovative antibody conjugation*. Retrieved from https://hdl.handle.net/1887/4273517

Version: Publisher's Version

Licence agreement concerning inclusion of doctoral

License: thesis in the Institutional Repository of the University

of Leiden

Downloaded from: <a href="https://hdl.handle.net/1887/4273517">https://hdl.handle.net/1887/4273517</a>

**Note:** To cite this publication please use the final published version (if applicable).



# Total Chemical Synthesis of a Functionalized GFP Nanobody

5

Published in:

A.F. Elhebieshy\*, Y. Huppelschoten\*, et al. Total Chemical Synthesis of a Functionalized GFP Nanobody. ChemBioChem 23, e202200304 (2022).



# **Total Chemical Synthesis of a Functionalized GFP Nanobody**

Angela F. Elhebieshy, Yara Huppelschoten, Dharjath S. Hameed, Aysegul Sapmaz, Jens Buchardt, Thomas E. Nielsen, Huib Ovaa and Gerbrand J. van der Heden van Noort.

#### **Abstract**

Chemical protein synthesis has proven to be a powerful tool to obtain homogenously modified proteins. The chemical synthesis of nanobodies (Nbs) would open up opportunities to design tailored Nbs with an array of chemical modifications such as tags, reporter groups, and small molecules. In this study, we describe the total chemical synthesis of a 123 amino-acid Nb targeting GFP. We applied a native chemical ligation—desulfurization strategy to successfully synthesize this GFP Nb, modified with a propargyl (PA) moiety for on-demand functionalization. Biophysical characterization indicated that the synthetic GFP Nb-PA was correctly folded after internal disulfide bond formation. Subsequently, we functionalized the synthetic Nb with either a biotin or a sulfo-Cyanine5 dye by copper(I)-catalyzed azide-alkyne cycloaddition (CuAAC) chemistry, resulting in two distinct probes. We used these probes for functional *in vitro* validation of the synthetic Nb in pull-down and confocal microscopy applications.

#### Introduction

Camelid species produce unique heavy-chain IgG antibodies consisting of a single antigen-binding variable heavy-chain domain (V,H) only, also referred to as nanobodies (Nbs).<sup>1,2</sup> These Nbs have unique properties such as their small size (~15 kD), robustness, high solubility, and monomeric nature, making them ideal for structural, cell, and developmental biology research tools.<sup>3–8</sup> Moreover, their high affinity (nM range) for targets, easy tissue penetration, and low immunogenicity make them promising candidates for new therapeutics. 9,10 Accordingly, much interest has been raised in functionalizing Nbs for various applications such as diagnostic tools, Nb-drug conjugates, and bivalent Nb conjugates. 11 Traditionally, Nbs are produced via recombinant protein expression, which easily provides functional Nbs but limits modification possibilities that are often based on using NHS- or maleimide chemistry, resulting in unselective chemical labeling that could drastically compromise the affinity of the Nb towards its target. We imagined that the chemical synthesis of a Nb would accelerate the process of generating homogeneous Nb-conjugates, considering that the chemical synthesis of proteins offers greater freedom of modification with both natural and unnatural amino acids. 12 Many functional groups suitable for chemoselective labeling could be thus easily introduced at defined, non-interfering regions of the Nb through a synthetic approach. Furthermore, since the structure of Nbs is highly conserved, it is an attractive protein for generic chemical synthesis that could pave the way for a modular synthetic approach that, with minor customization, could be broadly applied to a multitude of nanobodies. The general Nb structure comprises nine  $\beta$ -strands organized in a four- and a five-stranded  $\beta$ -sheet forming the conserved framework regions (FRs), connected via the complementarity determining region (CDR) loops and a conserved disulfide bond (Fig. 1). <sup>13,14</sup> The specificity for its target is obtained through the three CDRs at the ends of the variable domains. The long CDR3 loop contributes the most significantly to the specificity and affinity of the Nb. As a proof-of-concept, we selected a nanobody against GFP (referred to hereafter as GFP Nb), aiming to validate a synthetic approach that could prove useful within multiple applications. <sup>15</sup>

Considering the importance of the N-terminal clustering of the CDR loops in the affinity of Nbs towards their targets (Fig. 1), we envisioned that incorporating a propargyl moiety at the C-terminus would be ideal for later modifications using copper-mediated azide-alkyne cycloaddition (CuAAC) chemistry which uses mild, near physiological reaction conditions. <sup>16</sup> In this study, we present a native chemical ligation-based synthesis for the generation of a functionalizable GFP Nb. The on-demand conjugation of the synthetic Nb results in easy access to Nb-conjugates in a versatile manner. We applied this for the conjugation of either an affinity tag or a fluorescent moiety, which we used for pull-down and confocal microscopy experiments, respectively.

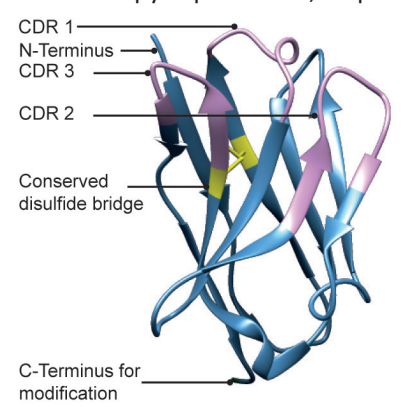


**Figure 1**| Structure of GFP Nb (PDB: 30GO). Indicated are the CDR domains in purple, the conserved disulfide bridge in yellow, and the C-terminus as a point of modification.

#### Results and discussion

#### Total chemical synthesis of GFP-Nb

Although the GFP Nb is relatively small, containing 123 amino acids, the  $\beta$ -sheet-rich structure is known to increase the likelihood of aggregation, on-resin and in-solution, during Fmoc-based solid-phase peptide synthesis (SPPS). Initial investigations proved that a three-segment NCL approach was necessary for the synthesis of the GFP Nb. The GFP Nb contains two native Cys residues, of which only one, however, is located at an appropriate potential ligation position (Cys<sub>97</sub>)(Fig. 2A). Therefore, NCL-desulfurization chemistry was chosen to assemble the Nb as an Ala-to-Cys mutation could facilitate a

NCL position that could be converted back to the native Ala using radical desulfurization post NCL. Accordingly, we envisioned using the acetamidomethyl (Acm) group to protect the other native Cys and prevent unwanted thioesterification or desulfurization during the construction of the GFP Nb. Our strategy for the synthesis of GFP Nb is outlined in Figure 2B, where we divided the polypeptide sequence into three fragments. Thioester fragment GFP Nb<sub>1-49</sub> (1), hydrazide fragment Cys-GFP Nb<sub>50-96</sub> (2), and Cys-GFP Nb<sub>97-123</sub> (4) were all prepared according to Fmoc-SPPS strategy on hydrazide or 2-chlorotrityl resins.  $^{19}$ 

Peptide **1** and **2A** were prepared as hydrazides for subsequent (*in-situ*) activation and thiolysis. Peptide **1** was synthesized with a final yield of 9 % (Fig. S1). For the synthesis and purification of peptide **2**, four pseudo-proline building blocks were incorporated during SPPS (underscored in Fig. 2A and Table S2), and the Fmoc was retained at the N-terminus of the peptide to enhance purification efficiency, resulting in 13% yield for **2A** (Fig. S2). Peptide **4** was synthesized with a GT iso-acyl dipeptide (underscored in Fig. 2A) incorporated to increase the solubility and improve the purification process, resulting in pure peptide (7% yield)(Fig. S3).

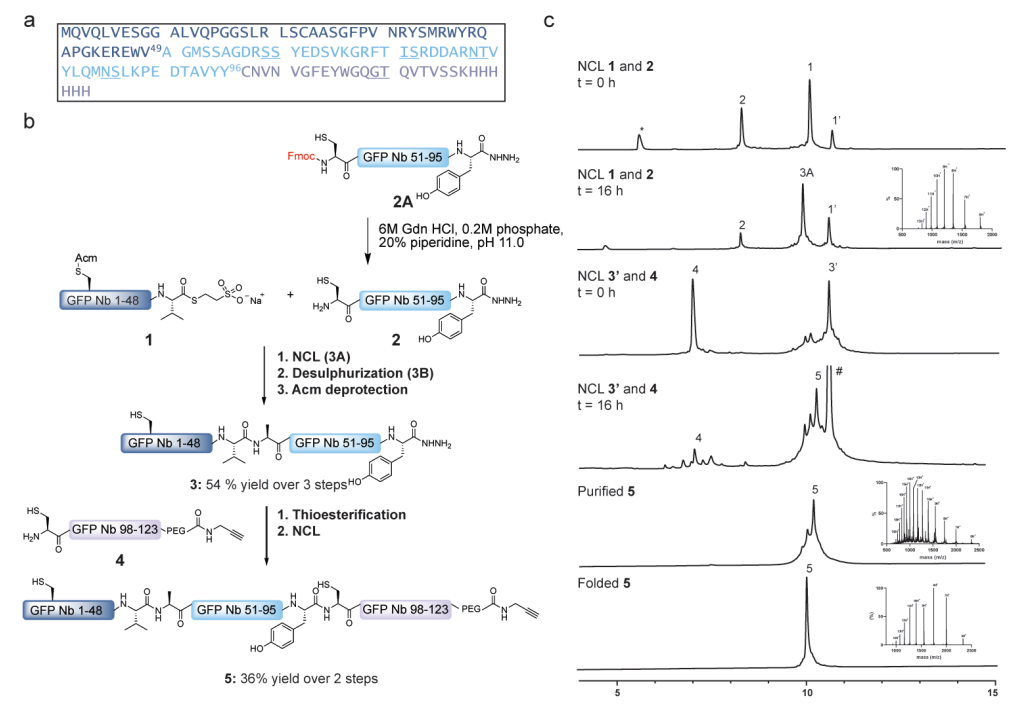


**Figure 2** (a) Sequence of GFP Nb, with underlined pseudo-proline dipeptides and iso-acyl dipeptides used in SPPS. (b) Synthetic strategy for obtaining GFP Nb. The complete synthetic approach is shown in Scheme S1-5 in the supplementary information. (c) UPLC analysis of the NCL of 1 and 2, the NCL of 3 and 4, purification of 5 and folding of 5. 'indicated MPAA thioesters, \* indicates dibenzofulvene adduct, # indicates MPAA disulfide adduct.

For the NCL of peptide **1** with peptide **2**, we used a one-pot Fmoc deprotection and NCL strategy described by Kar et al.<sup>20</sup> via *in-situ* preparation of **2** from **2A** (Fig. 2C, S4 and S5). After NCL between **1** and **2**, the Cys residue in the resulting conjugate was desulfurized to yield the native Ala residue, followed by an Acm deprotection step to liberate the N-terminal Cys leading to **3**. The one-pot thioesterification of **3** and ligation to **4**, yielded final GFP Nb product **5** that was obtained in 36% yield after HPLC purification (Fig. 2C, Fig.S8-9).

#### Chemically synthesized GFP Nbs show comparable folding to expressed GFP Nbs

With the full-length GFP  $Nb_{1-123}$ -linker-PA in hand, we continued to the folding step, including disulfide bond formation. The folding was carried out by stepwise dialysis in phosphate buffered saline (PBS). Spontaneous disulfide formation did not occur within 48 hours in PBS, so 2,2'-Dithio-dipyridin (DTP) $^{21,22}$ , a known disulfide bond formation accelerator, was added. Indeed, after the addition of 1 mM DTP to the folding buffer, initiation of disulfide bond formation was observed after 1 hour and completed within 16 hours, as observed in the high-resolution mass spectrum by the loss of 2 Da (Fig 3A, 3B and S10). To confirm the proper folding of the chemically synthesized and folded GFP Nb (5), we conducted circular dichroism (CD) experiments. The synthetic GFP Nb exhibited absorptions of  $\beta$ -sheet structures similar to the recombinantly expressed GFP Nb<sup>15</sup>, indicating that their folding is comparable (Fig. 3C).

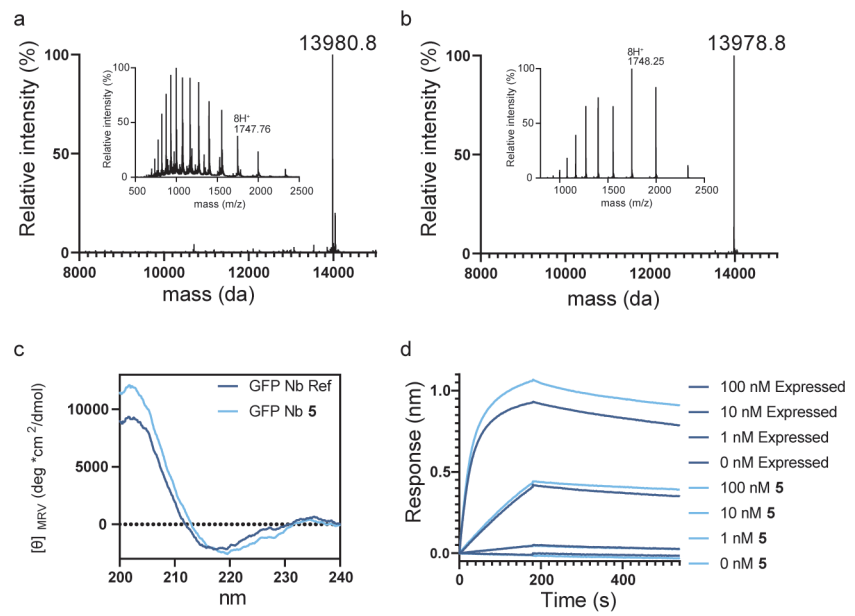


**Figure 3** (a) Deconvoluted mass spectrum and ESI Mass spectrum (inset) of unfolded 5. (b) Deconvoluted mass spectrum and ESI Mass spectrum (inset) of folded 5. (c) Circular dichroism spectra comparing recombinant and synthetic GFP Nb. (d) Bio Layer Interferometry analysis of folded 5 in comparison to expressed GFP Nb.

#### Chemically synthesized GFP Nbs retain antigen-binding affinity

To determine the affinity of the synthetic GFP Nb **5** to its target protein GFP and compare it to that of the recombinantly expressed GFP Nb, biolayer interferometry (BLI) experiments were performed. The C-terminal His-tag on both the expressed and synthetic Nb was used to immobilize the Nbs on Ni-NTA biosensor tips, and untagged GFP was used as the analyte at concentrations ranging from 1 nM to 100 nM. With this setup, the expressed and synthetic GFP Nb showed similar binding profiles (Fig 3D) and affinities of 1.12 and 1.11 nM, respectively. These values are in agreement with previously reported data in literature (1.4 nM).<sup>15</sup>

#### On-demand functionalization of GFP Nb-PA

Next, we wanted to show the adaptability of the fully synthetic Nb as a chemical tool by modifying the C-terminal propargyl moiety using a bio-orthogonal labeling strategy. Accordingly, we used copper(I)-catalyzed alkyne-azide cycloaddition (CuAAC) chemistry to functionalize the synthetic Nb with an azide-functionalized biotin molecule for the purpose of pull-down experiments (Fig. 4A). Unfolded, purified 5 was reacted with biotin-azide using mild reaction conditions (3 mM CuSO,, 10 mM sodium ascorbate, and 2 mM tris-(hydroxypropyltriazolylmethyl)amine (THPTA)) to form the GFP Nb-biotin conjugate (6) (Fig. S11). After the CuAAC, the synthetic Nb was folded as described previously for compound 5, removing all additives from the CuAAC reaction during the dialysis step. In addition, we envisioned that modification of 5 with sulfo-Cyanine5azide (Cy5) would lead to the opportunity to validate the proper functioning and target binding of our Nb by co-localization of the Nb with GFP-tagged proteins in cells using confocal microscopy. Hence, we used the same procedure to synthesize a GFP Nb-Cy5 conjugate (7)(Fig. S12). Next, we measured CD to warrant the correct folding of the functionalized Nbs (Fig. 4B, S13) and continued with CD denaturing experiments to investigate the stability of the synthetic Nb-conjugates carrying two different payloads compared to the expressed GFP Nb. Both Nb-conjugates showed a similar denaturing pattern as the expressed GFP Nb, indicating that the introduction of C-terminal cargo onto the Nb did not alter its biophysical properties (Fig. S14-S16).

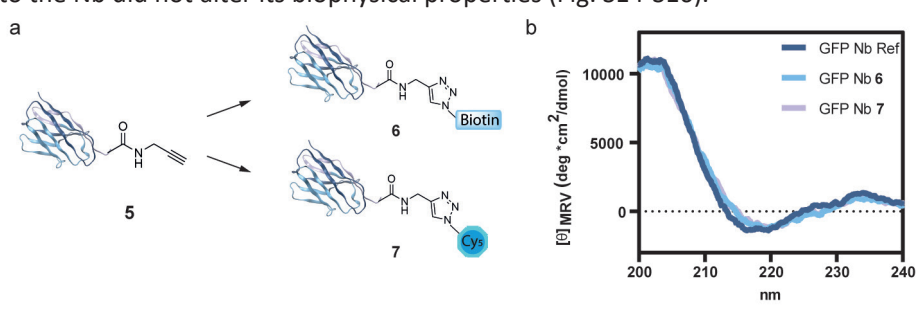


**Figure 4** (a) Functionalization of synthetic Nb 5. Nanobody structure PDB:3OGO17 (b) Circular Dichroism of expressed GFP Nb, synthetic GFP Nb conjugates 6 and 7.

#### Synthetic GFP Nb is functional as an in vitro research tool

Next, we wanted to assess the functionality of Nb conjugates **6** and **7** as research tools in *in vitro* assays for the recognition of GFP-labeled proteins. First, we set out to validate the binding of the synthetic GFP Nb to GFP-fusion proteins in a complex protein mixture by performing a pull-down assay. For this purpose, we decided to use the MelJuSo cell line established in our lab<sup>23</sup> that stably expresses GFP-tagged small GTPase Rab7, a central regulator of membrane trafficking in multiple directions.<sup>24</sup> Hence, we incubated the GFP Nb-biotin conjugate (**6**) with cell lysate of MelJuSo cells expressing GFP-Rab7 to perform a pull-down assay. To ensure GFP-specific binding, we used WT MelJuSo cells that did not express GFP-Rab7 as a negative control. After two hours of incubating conjugate **6** with the cell lysates of both GFP-Rab7 MelJuSo or WT MelJuSo, we were able to selectively pull down the GFP-Rab7 protein from the cell lysate showing a signal around 55 kDa, equal to the molecular weight of GFP-Rab7 (Fig. 5A). Negligible background signal confirms the selectivity of the synthetic GFP Nb for GFP over other proteins present in the cell lysate (Fig. S18).

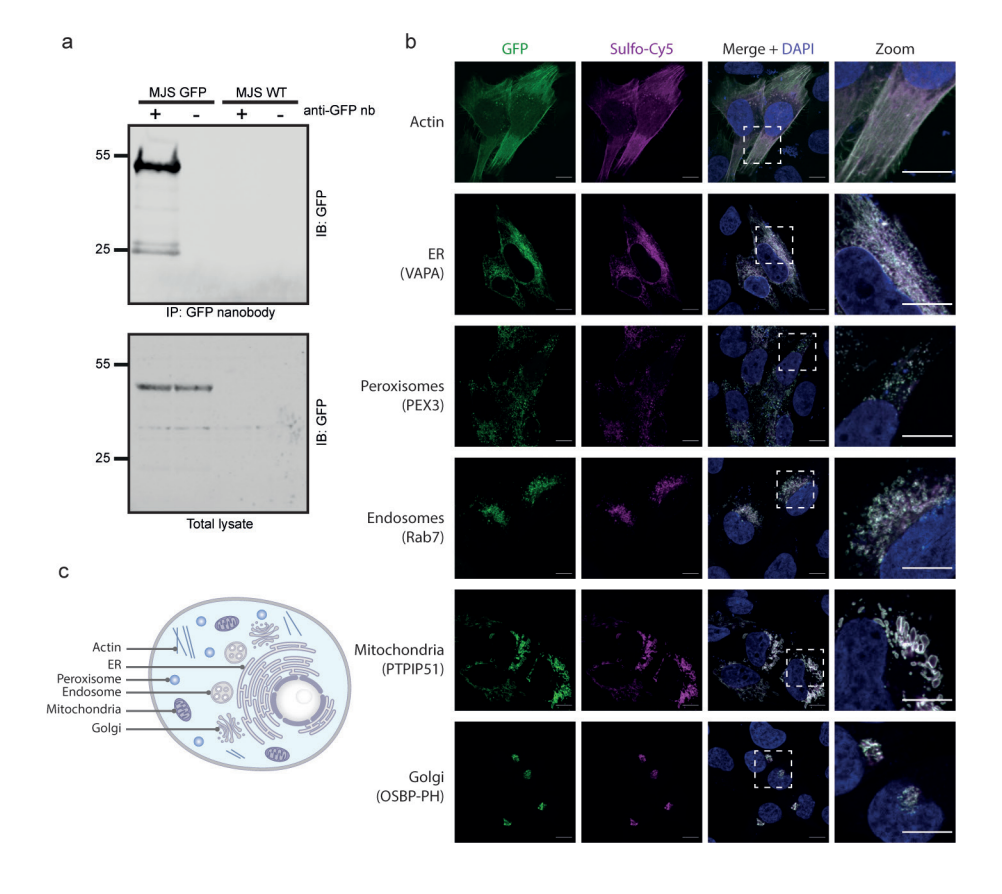


**Figure 5** (a) Western blot analysis of the pull-down of GFP-Rab7 from cell lysate using GFP Nb-biotin conjugate 6. The signal around 25 kDa is GFP as a result of protein degradation. (b) Confocal images of MelJuSo cells expressing GFP-Rab7 in the presence of GFP Nb-Cy5 7. (c) Illustration of a cell highlighting the cellular compartments visualized in B.

We also tested the synthetic GFP Nb in a confocal microscopy setting, where we used GFP Nb-Cy5 conjugate **7** to examine co-localization with GFP-tagged proteins located in different cellular compartments (cytoskeleton, endoplasmic reticulum (ER), peroxisomes, endosomes, mitochondria, and golgi). For this, MelJuSo cells were transfected with six different plasmids encoding for GFP tagged Actin, VAMP-Associated Protein A (VAPA), Peroxisomal biogenesis factor 3 (PEX3), Rab7, Protein tyrosine phosphatase interacting protein 51 (PTPIP51) and Oxysterol binding protein (OSBP-PH) proteins (Fig. 5B and C). The cells were fixed, and the membranes were permeabilized before incubation with the conjugate **7** for 1 hour. The incubation of the transfected MelJuSo cells with **7** resulted in a complete overlap between the GFP signal and the Cy5 signal, indicating the colocalization of the synthetic Cy5-Nb with the GFP tagged proteins (Fig. 5B). The staining with conjugate **7** resulted in a strong signal in each of the tested cell compartments with minimal background, indicating full target engagement of our synthetic Nb (Fig. 5B). The ability to visualize GFP fusion proteins at various cellular locations further efficiently showcases the broad applicability of the synthetic Nb.

#### Conclusion

In conclusion, we have developed a practical native chemical ligation-based synthetic approach for the generation of a synthetic GFP Nb ready for on-demand functionalization. With this method, we can obtain homogenous batches of labeled Nb by selectively labeling the Nb using CuAAC without altering the properties of the Nb, such as folding or thermo-stability. This technology was successfully applied to modify the GFP-Nb with either a biotin or a fluorophore, which were used in pull-down and confocal microscopy experiments, respectively. The Nb labeling is performed without compromising the antigen-binding site, making this method also applicable for Nbs containing a Cys residue in their CDR domains, that could be jeopardized during conventional maleimide based modification strategies. In addition, easy modification of the CDR3 domain can be obtained because it is introduced in one of the final synthesis steps in our native chemical ligation based synthesis scheme. We envision that with this protocol in hand, Nbs against other targets can be synthesized using a similar strategy due to the high sequence and structure similarities between Nbs. This methodology could potentially also be applied to the streamlined preparation of Nb drug-conjugates or (heterogeneous) Nb multimers. Moreover, unnatural amino acids can be easily introduced through the SPPS protocol, e.g. to confer stability of the Nb against degradation in vivo and broaden the applicability of this protein scaffold. 25,26

#### **Methods**

#### **General procedures**

#### **Materials and solvents**

Reagents were obtained from Sigma-Aldrich of the highest available grade and used without further purification. Standard Fmoc-protected amino acid derivatives were used and purchased from Gyros Protein Technologies unless mentioned otherwise. Fmoc-Cys(Acm)-OH and resins for SPPS were obtained from Novabiochem (Merck Millipore), Apigenex and PCAS Biomatrix. Pseudo-proline dipeptides were obtained from Corden Pharma or Bachem. Iso-acyl dipeptides were obtained from AAPPTec. Solvents for SPPS were obtained from Biosolve. VA-044 was procured from Wako Pure Chemical Corporation. Oxyma Pure® was purchased from Gyros Protein Technologies. HPLC grade acetonitrile was obtained from Merck.

#### **Analytical methods**

#### LC-MS conditions

LC-MS measurements were performed on a Waters Acquity UPLC H Class system, Waters Xevo G2-XS QTof with a Waters Acquity BEH 300 Å, C4, 1.7  $\mu$ m, 2.1 mm x 50 mm (0.4 mL/min). Samples were run at 60 °C using 3 mobile phases: A = 0.1 % formic acid in MilliQ water, B = 0.1 % formic acid in acetonitrile and C = 0.01 % TFA in MilliQ water with a gradient of 5 to 25% B over 1 min, 25 to 65 % B over 6 min followed by 65 to 95 % B over 0.5 min maintaining a composition of 5% C throughout. Data processing was performed using Waters MassLynx Mass Spectrometry Software V4.2 (deconvolution with MaxEnt I function).

#### **Analytical UPLC conditions**

UPLC measurements were performed on a Waters Acquity UPLC H Class system with a Waters Acquity BEH 300 Å, C4, 1.7  $\mu$ m, 2.1 mm x 100 mm (0.4 mL/min). Samples were run at 40 °C using 2 mobile phases: A = 0.05 % TFA in MilliQ water and B = 0.05 % TFA in acetonitrile with a gradient of 5 to 50 % B over 20 min followed 50 to 95% B over 0.5 min. Data processing was performed using Empower software.

#### Quantification

#### **Charged Aerosol Detection (CAD)**

Purified samples were quantified using a Thermo Scientific Vanquish, Corona Veo CAD. Samples were run on a Acquity BEH 300 Å, C4, 1.7  $\mu$ m, 2.1 mm x 50 mm at 40 °C using 2 mobile phases: A = 0.1 % TFA in MilliQ water and B = 0.1 % TFA in acetonitrile with a gradient of 0 to 80 % B over 7 min.

# Solid Phase Peptide Synthesis (SPPS) Preloading 2-chlorotrityl resin

2-Chlorotrityl resin (0.57 mmol/gram) was swollen in dry DCM for 30 minutes. A solution of Fmoc-AA-OH (1 equiv.) in dry DCM and DIPEA (4 equiv.) was added, and the resin was shaken for 30 minutes. The resin was washed with DCM twice before capping the remaining trityl groups with methanol/DIPEA/DCM 17:2:1, v/v/v. The resin was dried *in vacuo* prior to the determination of the estimated loading of the first amino acid.

#### **Automated Fmoc SPPS**

SPPS was performed on a Symphony X (Gyros Protein Technologies) automated peptide synthesizer using standard 9-fluorenylmethoxycarbonyl (Fmoc) based SPPS. Fmoc deprotection was achieved with 2 x 10 min. treatment of 20 vol. % piperidine, 0.1 % Oxyma Pure® in DMF. Peptide couplings were performed using DIC/Oxyma. Amino acid/Oxyma solutions (0.3 M/0.3 M in DMF) were added to the resin at 4-6-fold excess together with equal equivalents of DIC (1.5 M in DMF). The coupling time was 2 hours unless specified otherwise. All dipeptide building blocks were coupled for 4 hours. The residual free amino groups after the coupling reaction were capped by the addition of collidine (3.3 equiv., 1.5 M in DMF) and acetic anhydride (11 equiv., 1.0 M in DMF) and were reacted for 20 minutes. After the final Fmoc deprotection the resin was washed with DMF and DCM.

#### Global deprotection from the resin and side chain deprotection

Polypeptide sequences containing a cysteine residue were detached from the resin and deprotected by treatment with Reagent K (TFA/phenol/H<sub>2</sub>O/thioanisole/EDT, 82.5:5:5:5:2.5 v/v/v/v/v) for 2-3 hours followed by precipitation in ice cold diethylether and collection by centrifugation. Polypeptide sequences containing methionine residues were detached from the resin and deprotected by treatment with TFA/TIPS/H<sub>2</sub>O/DCM/NH<sub>4</sub>I/DTT, 87:5:2.5:2.5:0.5:2.5, v/v/v/v/v for 2-3 hours followed by precipitation in ice cold diethylether and collection by centrifugation. The pellet was resuspended in diethylether before being collected by centrifugation again. The pellet was dissolved and lyophilized from H<sub>3</sub>O/CH<sub>3</sub>CN/AcOH, 65:25:10, v/v/v before purification.

#### **Preparative HPLC purification**

Preparative purification was performed on a Gilson HPLC system using a reversed phase HPLC column as specified in the experimental section. Elution was performed using 2 mobile phases: A =  $0.1\,\%$  TFA in MilliQ water and B = 0.1% TFA in acetonitrile using a linear gradient. Fractions were collected using a Gilson fraction collector. Relevant fractions were assessed by LC-MS and pure peptide was pooled and lyophilized.

#### Nanobody characterization

The construct for GFP Nb was obtained from addgene (49172) and expressed as described previously by Kubala et al.<sup>15</sup> In brief, protein expression was conducted in E. coli strain BL21(DE3) in a flask containing LB medium and grown to an OD<sub>600</sub> of 0.5 at 37°C, and then, protein expression was induced using 0.5 mM IPTG. Further fermentation was carried out at 20°C for 20 h. Resultant cell mass was harvested by centrifugation, disrupted by sonication, and subjected to centrifugation to remove cell debris. The cleared cell lysate was subjected to HisTrap affinity purification followed by size-exclusion fractionation (Superdex 75) using an Akta Purifier FPLC system (GE Healthcare).

#### Cell culture and pull-down of overexpressed GFP-Rab7

MelJuSo (human melanomas) cell lines stably expressing GFP-Rab7 were kindly gifted by A. Sapmaz (LUMC, Leiden) and WT MelJuSo cells, kindly provided by Prof. G. Riethmuller (LMU, Munich).  $^{23}$  The cells were lysed in lysis buffer (0.8 % NP40, 150 mM NaCl, 50 mM Tris-HCl pH 8.0, 0.05 mM MgCl $_{\rm 2}$  + protease inhibitor) followed by brief sonication. Cell debris was removed by centrifugation. Next, 5 µg of biotin tagged synthetic GFP Nb was added to cell lysates of both GFP-Rab7 expressing cells and WT cells and incubated by rotating for 2 hours at 4 °C. Thereafter, high capacity neutravidin beads (Thermo Scientific, Cat# 29202) were added and incubated by rotating for 1 hour at 4 °C. The beads were extensively washed with lysis buffer and after completely removing the washing buffer, SDS sample buffer supplemented with 2-mercaptoethanol was added to the beads and boiled at 95°C. The proteins were separated by SDS-PAGE followed by western blotting and detection by ponceau s followed by antibody staining using rabbit anti-GFP antibody  $^{27}$  followed by IRDye 800CW goat anti-rabbit IgG (H + L) (Li-COR, Cat# 926-32211). The signal was detected using direct imaging by the Odyssey Classic imager (LI-COR).

#### **Confocal microscopy**

MelJuso cells were seeded into 24-well plates containing glass coverslips to achieve 40-50% confluency the following day. Cells were transfected with the DNA plasmids in table 1 using X-tremeGENE HP (Roche Cat# XTGHP-RO) according to manufacturer's instruction and cultured for 18-24 hours. Next, the cells were fixed in 3.7% formaldehyde in PBS for 20 min and subsequently permeabilized using 0.1% Triton X-100 in PBS for 10 min. After permeabilization, cells were blocked using 5% (w/v) skim milk powder in PBS for 30 min and incubated with 1  $\mu$ g Cy5-labelled synthetic Nb (7) in blocking buffer for 1 hour at RT. Next, cells were washed and mounted using ProLong Gold antifade Mounting medium with DAPI (Life Technologies, Cat# P36941). Samples were imaged using Leica SP5 or SP8 microscopes equipped with appropriate solid-state lasers, HCX

PL 63x magnification oil emersion objectives and HyD detectors. Image processing and co-localization analyses were performed using the Fiji software.

Table 1. DNA plasmids used for transfection with the corresponding protein.

Protein	Cell compart- ment	Plasmid	Reference and cloning
RAB7A	Endosomes	GFP-RAB7A	28
VAMP-Associated Protein A (VAPA)	ER	GFP-VAPA	29
Peroxisomal biogenesis factor 3 (PEX3)	Peroxisomes	PEX3*-SBP-GFP	PEX3*-SBP-GFP was a gift from Juan Bonifacino  (Addgene plasmid # 120174).30
Protein tyrosine phosphatase interacting protein 51 (PTPIP51)	Mitochondria	PTPIP51-GFP	PTPIP51 ORF was cloned into GFP-C1 vector from PTPIP51-RFP using HindIII and BamHI restriction enzymes. <sup>29</sup>
Oxysterol binding protein (OSBP-PH)	Golgi	EGFP-OSBP-PH	EGFP-OSBP-PH was a gift from Marci Scidmore (Ad- dgene plasmid # 49571). <sup>31</sup>
LifeAct	Actin filaments	Lifeact-EGFP	Addgene Plasmid # 58470

#### **Bio Layer Interferometry-measurements**

BLI measurements were performed on an OctetRed system (ForteBio). 100 nM of the expressed GFP Nb or the synthetic GFP Nb were loaded on Ni-biosensors for 2 minutes and washed in binding buffer (phosphate-buffered saline (PBS), 0.05 % Tween-20, 0.01 % BSA, pH 7.4). Thereafter, the sensors were transferred into solutions containing varying concentrations of GFP (100 - 1 nM) to measure the association of the analyte for 3 minutes. Subsequently, the dissociation of the complex was measured in binding buffer for 6 minutes. Dissociation constants (Kd) were calculated using the ForteBio Data Analysis software by co-fitting all concentrations simultaneously.

#### **Acknowledgments**

We would like to thank Dr. Birol Cabukusta at the LUMC for plasmids used for confocal microscopy experiments. YH acknowledges funding from the European Union's Horizon 2020 research and innovation programme under the Marie Skłodowska-Curie grant agreement No 765445 (ITN UbiCODE), AFE acknowledges funding by ICI (grant No ICI00013) and GJvdHvN acknowledges funding by NWO (VIDI grant VI.192.011).

# **Supplementary information**

## **Synthesis strategy**

**Scheme S1.** Complete synthetic approach towards synthetic GFP Nb using NCL-desulfurization chemistry.

# Sequences GFP Nanobody:

- 1 MQVQLVESGG ALVQPGGSLR LSCAASGFPV NRYSMRWYRQ
- 41 APGKEREWVA GMSSAGDRSS YEDSVKGRFT ISRDDARNTV
- 81 YLQMNSLKPE DTAVYYCNVN VGFEYWGQGT QVTVSSKHHH HHH

**Table S2.** Amino acid sequences of the Nb fragments, psuedoprolines are underscored and iso-acyl dipeptides in bold.

Segment ID	SPPS sequence
GFP 1-48	H-MQVQLVESGGALVQPGGSLRLSC(Acm)AASGFPVNRYSMRWYRQAPG- KEREWV-NHNH <sub>2</sub>
Fmoc-GFP 49-96	H-CGMSSAGDR <u>SS</u> YEDSVKGRFT <u>IS</u> RDDAR <u>NT</u> VYLQM <u>NS</u> LKPEDTAVYY-NHNH <sub>2</sub>
GFP 98-123 OEG	H-CNVN <u>VG</u> FEYWGQ <b>GT</b> QVTVSSKHHHHHHHX-OH

X was incorporated as a Fmoc-Peg2-OH. Underlined dipeptide sequences were coupled as the respective pseudoproline dipeptides or DMB dipeptides. Italic dipeptides were coupled as the respective iso-acyl dipeptides.

# Preparation of peptide fragments Synthesis of GFP 1-48 thioester 1

The synthesis was performed following general procedures using 2-chlorotrityl hydrazine resin (1.0 gram, 0.32 mmol/gram). The peptide was cleaved from the resin according to the general procedures and purified by preparative HPLC using a Phenomenex, Luna 100 Å, C8(2), 10  $\mu$ m, 30 mm x 250 mm column (25 to 35%B over 20 min, 30mL/min). Peptide 1 was dissolved in 45 mL of 6 M Gdn.HCl pH 3.0 and 1 M NaNO $_2$  in MilliQ (3.2 mL, 3.2 mmol, 10 equiv.) was added and stirred for 15 min at 0 °C. The reaction was warmed to room temperature and MESNa (5.1 gram, 32 mmol, 100 equiv.) in 6 M Gdn.HCl, 0.2 M phosphate pH 7.0 was added. The pH was adjusted to pH 7.0 and the solution was stirred for 60 min. before purification by preparative RP-HPLC using Phenomenex, Luna 100 Å, C8(2), 10  $\mu$ m, 30 mm x 250 mm (22 to 32 % B over 45 min, 30mL/min) followed by lyophilization afforded peptide 1 as a white solid (171.6 mg, 9.3 % yield).

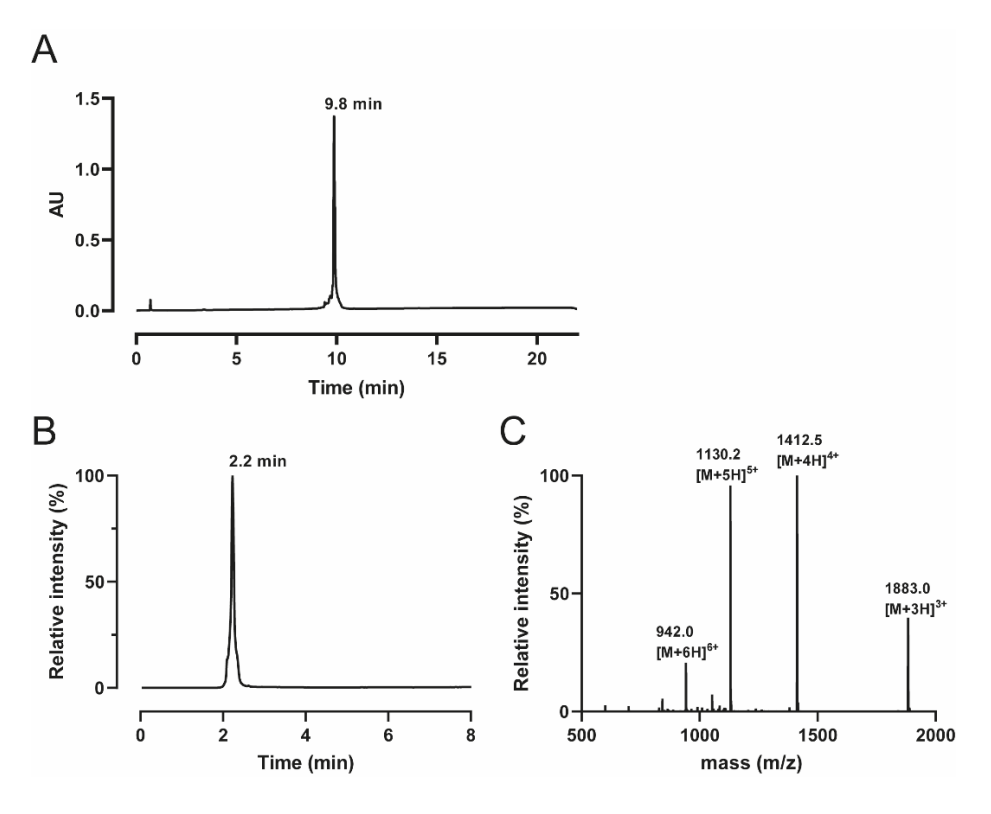


**Figure S1.** (A) UPLC UV chromatogram of purified 1, Rt 9.86 min. (B) Total ion chromatogram (LC-MS method C4) of purified 1, Rt 2.23 min. (C) Observed ESI spectrum of purified 1. Calculated Mass (average isotope composition): 5645.74; Observed:  $[M + 3H]^{3+}$ : 1882.9,  $[M + 4H]^{4+}$ : 1412.4,  $[M + 5H]^{5+}$ : 1130.1,  $[M + 6H]^{6+}$ : 941.9.

### Synthesis of Fmoc-GFP 49-96 hydrazide 2A

The synthesis was performed following general procedures using 2-chlorotrityl hydrazine resin (1.27 gram, 0.32 mmol/gram). The peptide was cleaved from the resin according to the general procedures and purified by preparative RP-HPLC using a Phenomenex, Luna 100 Å, C8(2), 10  $\mu$ m, 30 mm x 250 mm column (26 to 33 % B over 40 min, 30 mL/min) followed by lyophilization afforded peptide **2A** as a white solid (296.6 mg, 13.2% yield).

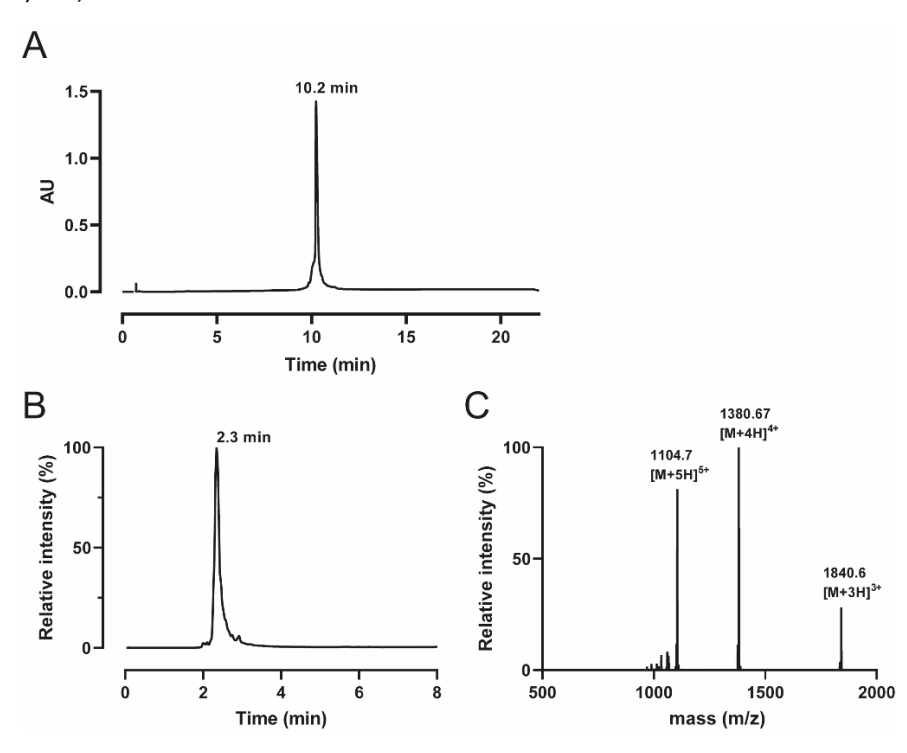


**Figure S2.** (A) UPLC UV chromatogram of purified 2A, Rt 10.23 min. (B) Total ion chromatogram (LC-MS method C4) of purified 2A, Rt 2.35 min. (C) ESI spectrum of purified 2A. Calculated Mass (average isotope composition): 5518.53; Observed: [M + 3H]<sup>3+</sup>: 1840.51, [M + 4H]<sup>4+</sup>: 1380.63, [M + 5H]<sup>5+</sup>: 1104.71.

#### Synthesis of GFP 98-123 propargyl amide 4A

The synthesis was performed following general procedures using Fmoc-OEG preloaded CTC resin (1.45 gram, 0.2 mmol/gram). The amino acids colored in red were coupled using single 6 hours coupling. For the underlined amino acids in the sequence an isoacyl dipeptide Boc-Thr(Fmoc-Gly)-OH was coupled following the general procedures. The iso-acyl dipeptide was incorporated to increase solubility of the peptide during purification.

#### **CNVNV**GFEYWGQGTQVTVSSKHHHHHH

The protected polypeptide was cleaved from the resin by treatment with 3 x 15 mL of DCM/HFIP 7:3 v/v for 15 min and filtered. The combined filtrates were concentrated *in vacuo* and co-evaporated with DCM 3x and dried under high vacuum. The protected peptide (1 equiv.) was dissolved in DCM (10 mL) and propargylamine (75  $\mu$ L, 1.16 mmol, 4 equiv.) was coupled using PyBOP (597 mg, 1.16 mmol, 4 equiv.) and DIPEA (396  $\mu$ L, 2.32 mmol, 8 equiv.) for 16 hours. Thereafter, the solvents were removed *in vacuo* and the protecting groups was cleaved according to the general procedures. The crude peptide was purified by RP-HPLC using Phenomenex, Gemini® 110 Å, C18, 5  $\mu$ m, 30 mm x 250 mm column (15-35 % B over 20 min, flow 30 mL/min) and lyophilized to afford the desired peptide (65.07 mg, 6.7 % yield).

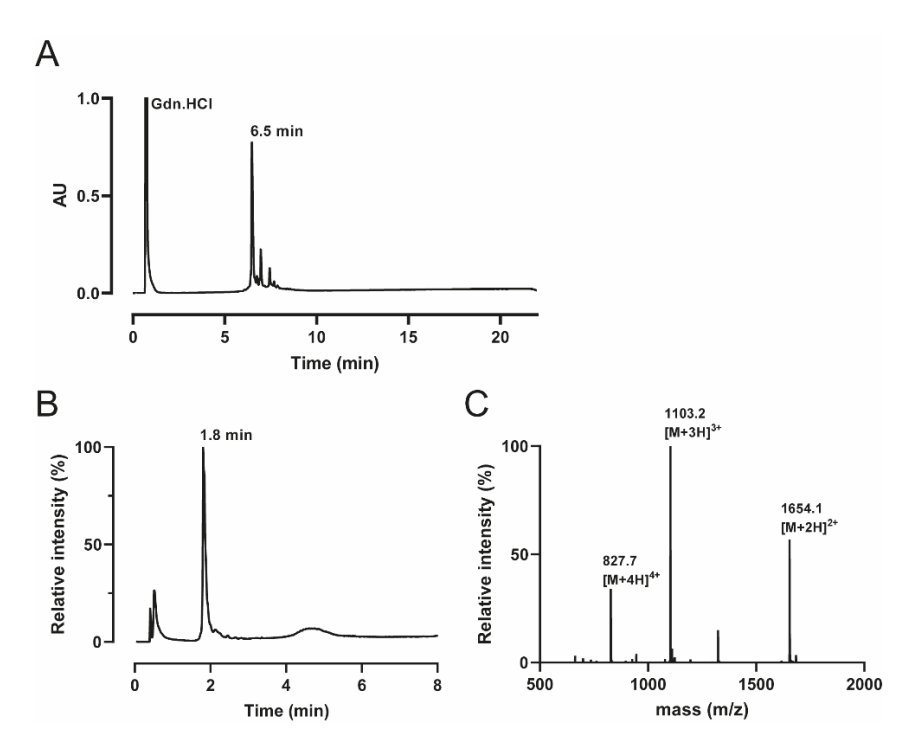


**Figure S3.** (A) UPLC UV chromatogram of purified 4, Rt 6.53 (B) Total ion chromatogram (LC-MS method C4) of purified 4, Rt 1.8 min. (C) ESI spectrum of purified 4. Calculated Mass (average isotope composition): 3306.52; Observed: [M + 2H]<sup>2+</sup>: 1654.26, [M + 3H]<sup>3+</sup>: 1103.17, [M + 4H]<sup>4+</sup>: 827.63

# Assembly of GFP Nb

#### One-pot Fmoc deprotection and ligation for the assembly of 3

Scheme S2. Fmoc deprotection of 2A.

A solution of **2A** (73.56 mg, 13.3 µmol) was prepared in 6 M Gdn.HCl, 0.2 M phosphate pH = 7.0 (5 mL), then 406 µL of conc. HCl was added and finally 1375 µL of piperidine, final pH of 10.7. The reaction mixture was shaken (350 rpm) for 10 min before the pH was adjusted to pH 7.0. The reaction progress was assessed by analyzing a small sample by LC-MS. Analysis revealed complete Fmoc deprotection within 10 min. to afford compound **2** in solution.

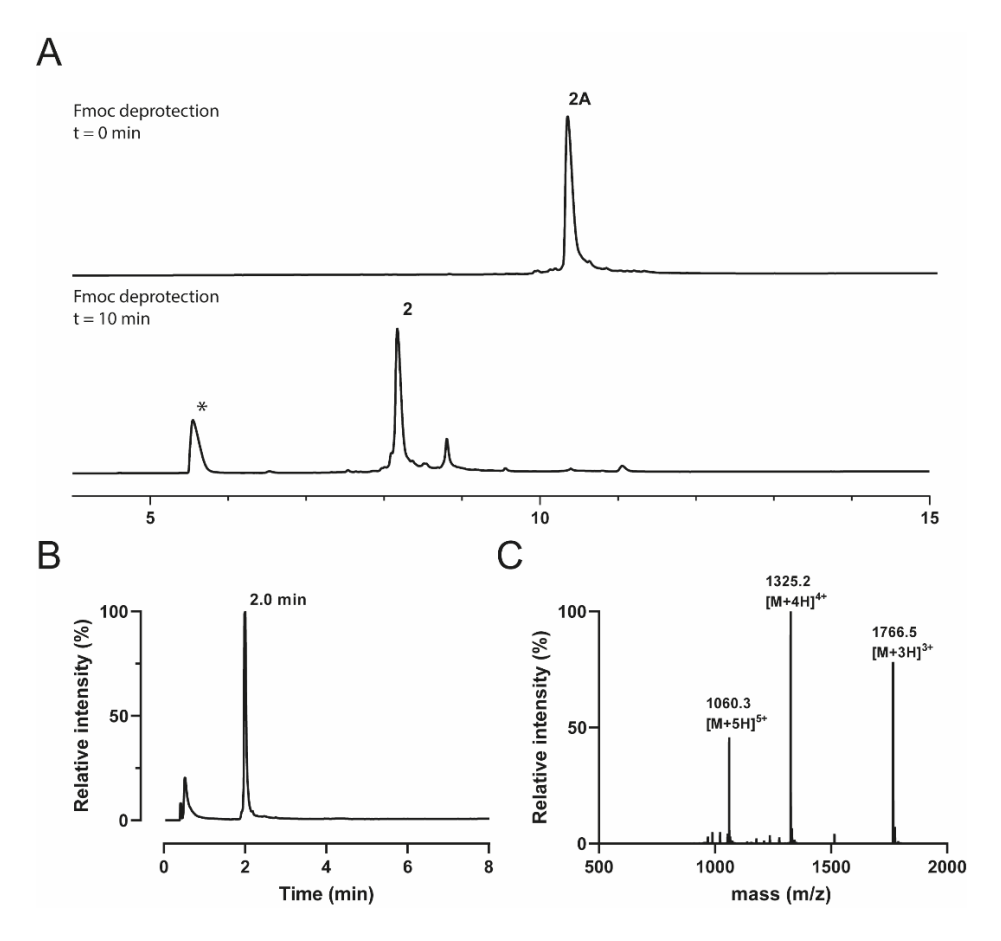
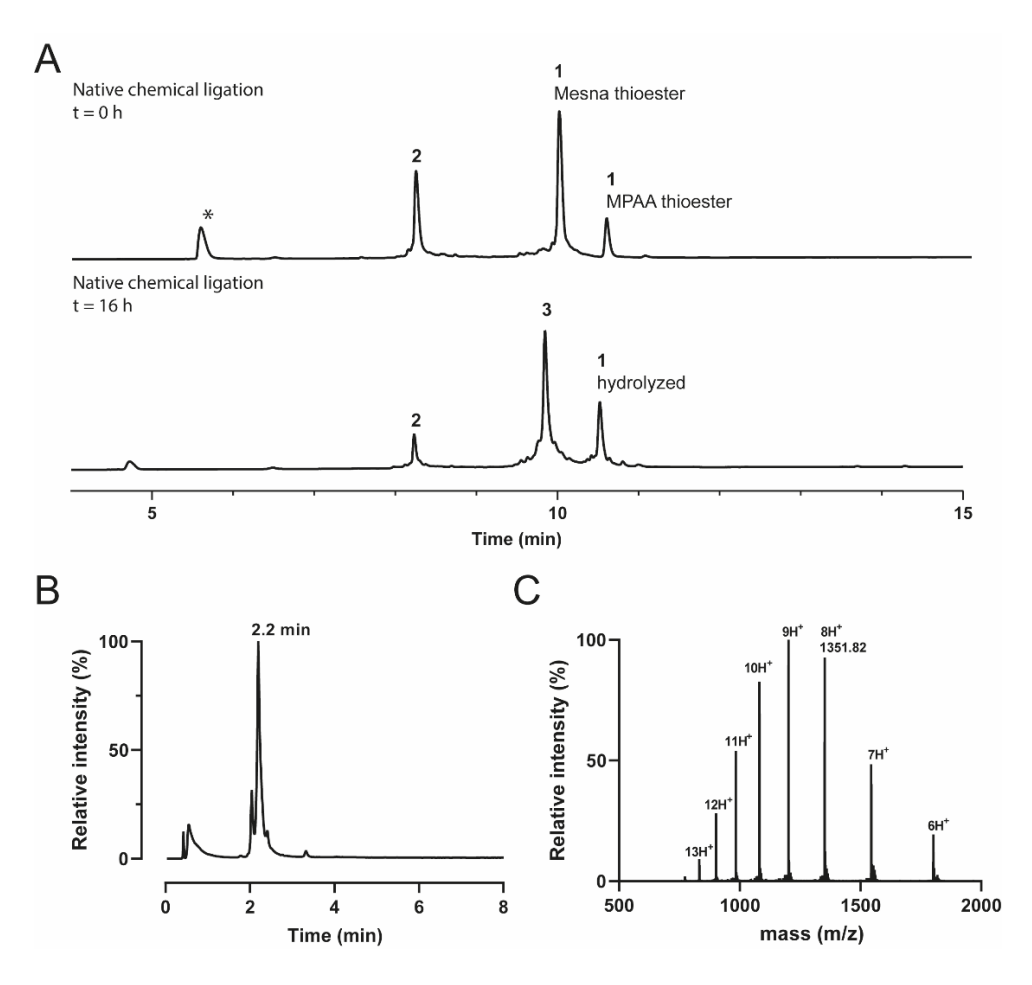


Figure S4. (A) UPLC UV chromatogram of the Fmoc deprotection of 2At = 0 min. (top chromatogram) and t = 10 min. (bottom chromatogram). \*dibenzofulvene-piperidine adduct (B) Total ion chromatogram (LC-MS method C4) of 2, Rt 2.0 min. (C) ESI spectrum of 2. Calculated Mass (average isotope composition): 5296.46; Observed:  $[M + 3H]^{3+}$ : 1766.48,  $[M + 4H]^{4+}$ : 1325.11,  $[M + 5H]^{5+}$ : 1060.29.

Scheme S3. Ligation of peptides 1 and 2 followed by desulfurization and Acm deprotection to assemble peptide 3.

Next peptide 1 (60.51 mg, 0.01286 mmol) was added as a solid to the reaction mixture containing 2. MPAA (186.4 mg, 1.1 mmol, 100 equiv.) was dissolved in 400 µL of 4 M NaOH and added to the reaction mixture and TCEP was added to a final concentration of 25 mM. The final pH was adjusted to 7.0 and the reaction was shaken for 16 hours at 37 °C upon which LCMS analysis showed that the reaction was complete. The MPAA was removed using a 3 kDa cut-off spin filter until LCMS no longer showed presence of MPAA. To the 6 M Gdn.HCl, 0.2 M phosphate pH = 7.0 solution (3 mL), 0.5 M TCEP in water (3 mL) was added and the solution was degassed with argon. To this solution glutathione (101.5 mg, 50 mM) and VA-044 (57 mg, 25 mM) were added and the reaction mixture was shaken at 40 °C for 18 hours at final pH 6.5. To afford peptide 3 in 101.6 mg with a 88 % yield over 2 steps. The buffer was exchanged again using a 3 kDa cut-off spin filter to 6 M Gdn.HCl, 0.2 M phosphate pH 7.0. Next PdCl<sub>3</sub> (29.6 mg, 20 equiv.) was added, and the reaction was shaken at 40 °C for 1 hour. To quench the reaction DTT (137.3 mg, 100 equiv.) was added and the solution was centrifuged. The supernatant was purified on an Äkta system using a HiLoad 26/600 Superdex 75 pg column (flow: 1 mL/min) to obtain GFP 1-96 in a solution of 6 M Gdn.HCl, 0.2 M phosphate, pH 7.0 (9.6 mg/mL, 62.2 mg, 61.7 % yield over 4 steps).

All concentrations/amounts were determined using CAD as described in the general protocols.



**Figure S5.** (A) UPLC UV chromatogram of the NCL of 1 and 2, t = 0 h (top chromatogram) and t = 16 h (bottom chromatogram). \*dibenzofulvene-piperidine adduct (B) Total ion chromatogram (LC-MS method C4) of 3, Rt 2.2 min. (C) ESI spectrum of 3. Calculated Mass (average isotope composition): 10800.22; [M + 6H]<sup>6+</sup>: 1801.04, [M + 7H]<sup>7+</sup>: 1543.89, [M + 8H]<sup>8+</sup>: 1351.03, [M + 9H]<sup>9+</sup>: 1201.02, [M + 10H]<sup>10+</sup>: 1081.02, [M + 11H]<sup>11+</sup>: 1081.02, [M + 11H]<sup>11+</sup>:

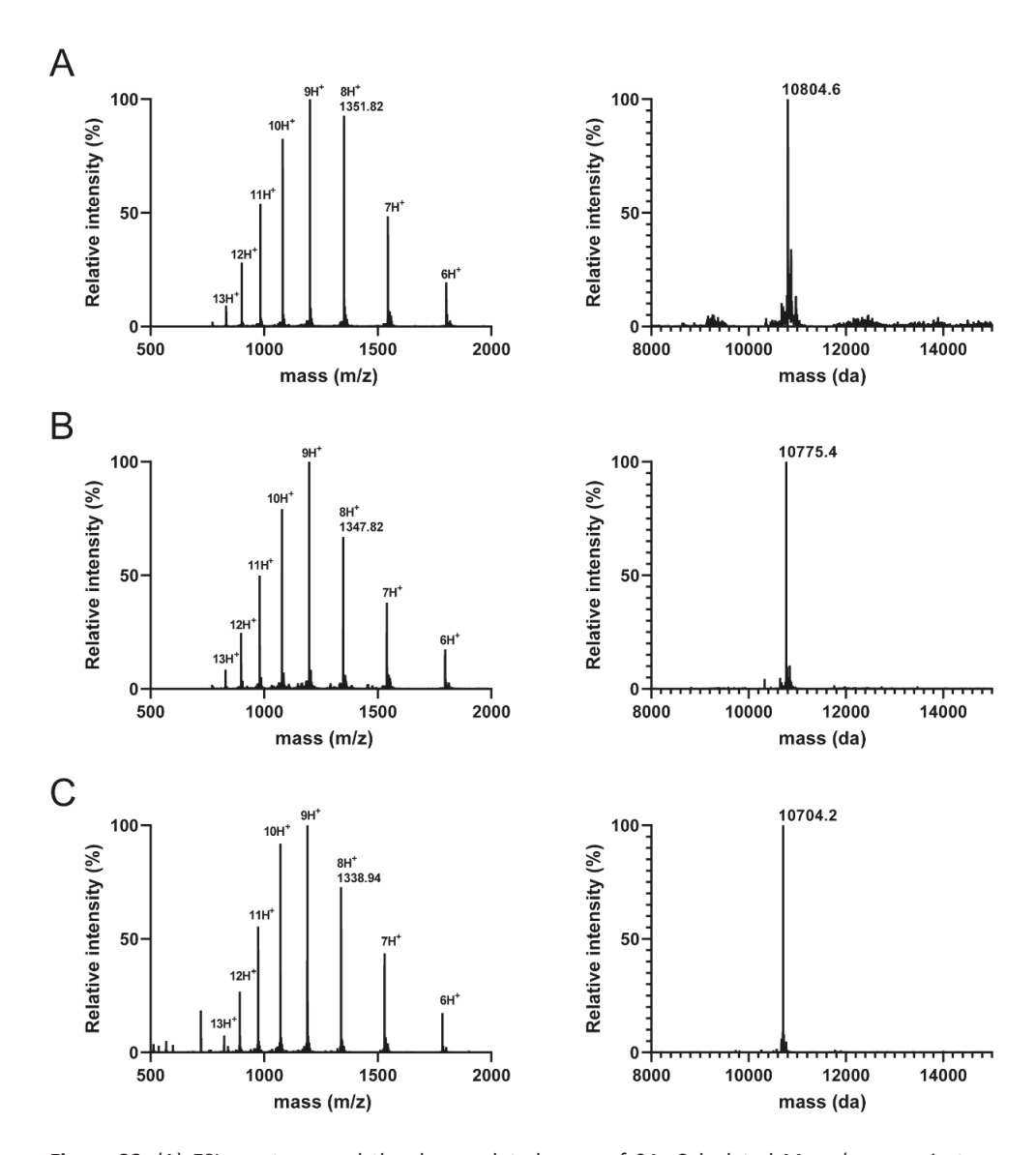


**Figure S6.** (A) ESI spectrum and the deconvoluted mass of 3A. Calculated Mass (average isotope composition):10800.22, Observed: 10801.52. Deconvoluted mass calculated: 10807.0, Observed: 10804.6 (B) ESI spectrum and the deconvoluted mass of 3B. Calculated Mass (average isotope composition): 10768.25, Observed: 10769.52. Deconvolute mas calculated: 10774.9, Observed: 10775.4. (C) ESI spectrum and the deconvoluted mass of 3 Calculated Mass (average isotope composition): 10697.21, Observed: 10698.4. Deconvolute mass calculated: 10703.9, Observed: 10704.2.

#### **Iso-acyl shift of 4A**

As described in the synthesis section of peptide **4A**, an iso-acyl dipeptide was incorporated to increase solubility during purification. The ester bond is not stable during NCL and therefore has to undergo an  $O \rightarrow N$  acyl shift to form the stable native peptide (Scheme S4).

Scheme S4. Shift of the iso-acyl dipeptide.

The peptide **4A** (9.4 mg, 2.8  $\mu$ mol) was dissolved in 400  $\mu$ L 6 M Gdn.HCl, 0.2 M phosphate, pH 7.4. After 10 minutes an UPLC sample was measured and the retention time of the peptide shifted from 6.47 to 6.96 minutes (UPLC method 2), indicating that the iso-acyl had shifted successfully (Fig. S7).

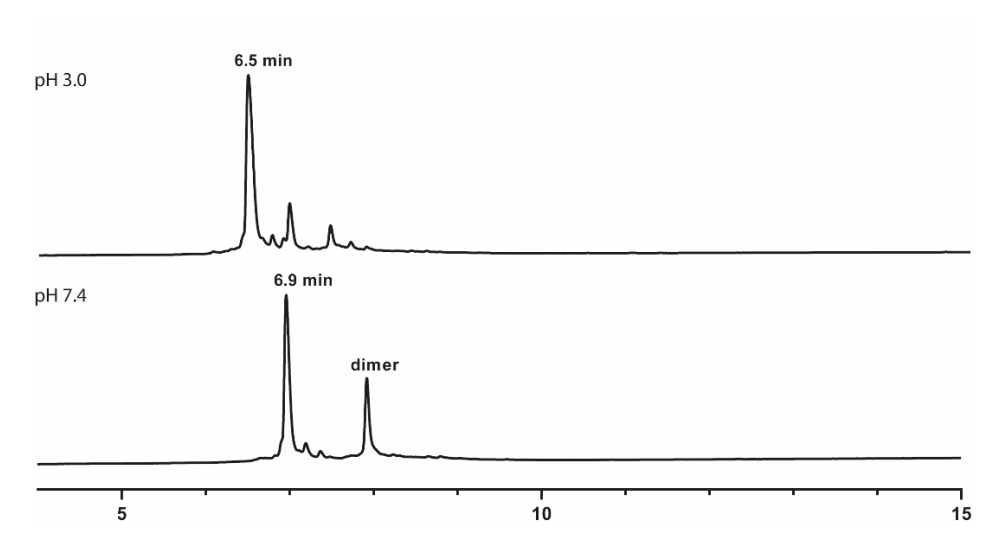


Figure S7. UPLC UV chromatogram of 4A at pH 3.0 (top chromatogram) and 4 at pH 7.4 (bottom chromatogram).

#### One-pot thioesterification and ligation to GFP 1-123-PA

Scheme S5. One-pot thioesterification and NCL of 3 and 4 to obtain the final product 5.

A solution of **3** (28.8 mg, 2.69  $\mu$ mol) in 3 mL of 6 M Gdn.HCl, 0.2 M phosphate, pH 3.0 was cooled to 0 °C before adding 27  $\mu$ L of 1 M NaNO<sub>2</sub> in MilliQ. After 15 minutes the solution was warmed to room temperature and MPAA (51 mg, 303  $\mu$ mol, 100 equiv.) in 4 M NaOH (50  $\mu$ L), and **4** (9.4 mg, 2.8  $\mu$ mol) were added, and the pH was adjusted to pH 7.13. The mixture was shaken over night at room temperature to reach completion

before purification on a Äkta system using a HiLoad\* 26/600 Superdex\* 75 pg column (flow: 1 mL/min) to obtain in a solution of 6 M Gdn.HCl, 0.2 M phosphate, pH 7.0 (9.13 mg/mL, 13.71 mg, 36.4 % yield based on recovered starting material).

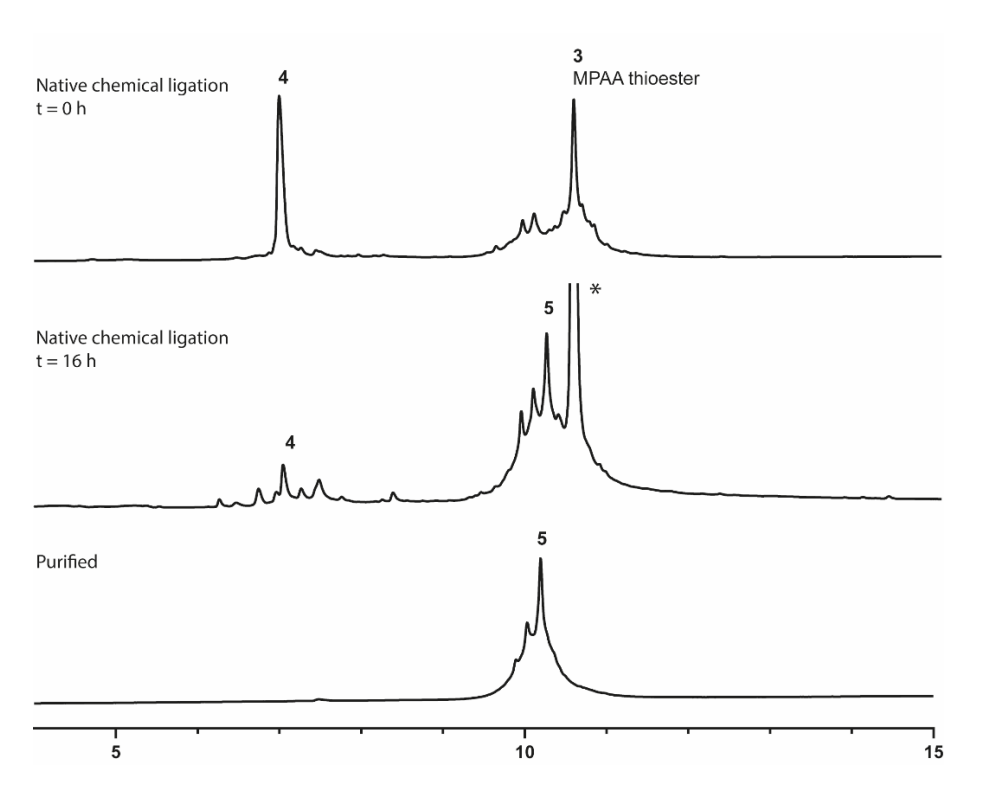


Figure S8. UPLC UV chromatogram of NCL between 4 and 3 t = 0 h (top chromatogram), t = 16 h (middle chromatogram), and purified 5 (bottom chromatogram)

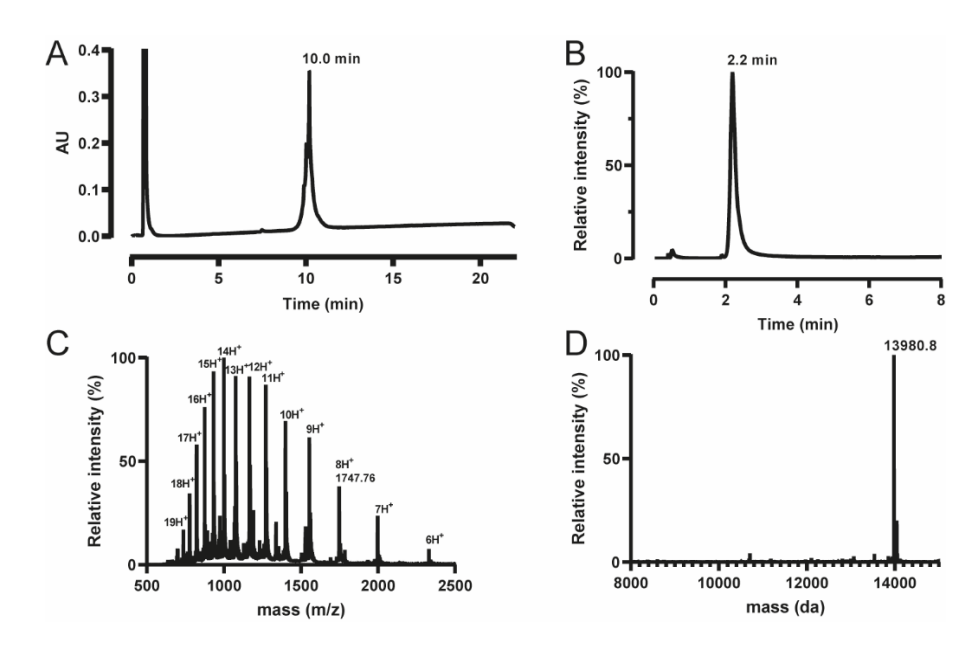


Figure S9. (A) UPLC UV chromatogram of 5, Rt 13.9 min. (B) Total ion chromatogram (LC-MS method C4) of 5, Rt 2.2 min. (C) ESI spectrum of 5. Calculated Mass (average isotope composition): 13971.70;  $[M+6H]^{6+}$ : 2329.62,  $[M+7H]^{7+}$ : 1996.95,  $[M+8H]^{8+}$ : 1747.46,  $[M+9H]^{9+}$ : 1553.41,  $[M+10H]^{10+}$ : 1398.17,  $[M+11H]^{11+}$ : 1271.16,  $[M+12H]^{12+}$ : 1165.31,  $[M+13H]^{13+}$ : 1075.75,  $[M+14H]^{14+}$ : 998.97. Observed: ;  $[M+6H]^{6+}$ : 2329.81,  $[M+7H]^{7+}$ : 1997.14,  $[M+8H]^{8+}$ : 1747.62,  $[M+9H]^{9+}$ : 1553.45,  $[M+10H]^{10+}$ : 1398.30,  $[M+11H]^{11+}$ : 1271.18,  $[M+12H]^{12+}$ : 1165.33,  $[M+13H]^{13+}$ : 1075.78,  $[M+14H]^{14+}$ : 999.00. (D) Deconvoluted mass of 5, calculated: 13980.4, observed: 13980.8.

#### Folding of 5

PBS buffer, pH 7.4 was freshly prepared from Gibco PBS tablets and sterilized with a bottle top vacuum filter, 0.22  $\mu$ m (Corning). A solution of crude unfolded **5** (0.65 mM, 1.5 mL) in 6 M Gdn.HCl, 0.2 M phosphate, pH 7.0 was added to a prewashed Slide-A-Lyzer<sup>TM</sup> MINI Dialysis Devices (3.5 kDa cut-off) containing 3 M Gdn.HCl 0.2 M phosphate, pH 7.0. After 2 hours the buffer was exchanged to PBS, pH 7.4 and the mixture was shaken gently over night at 10 °C. The mixture was analyzed by LC-MS revealing the correct MW corresponding to a loss of 2 Da. The mixture was concentrated using a prewashed centrifugal 3 kDa molecular weight cut-off device and concentrated to ~ 400  $\mu$ L.

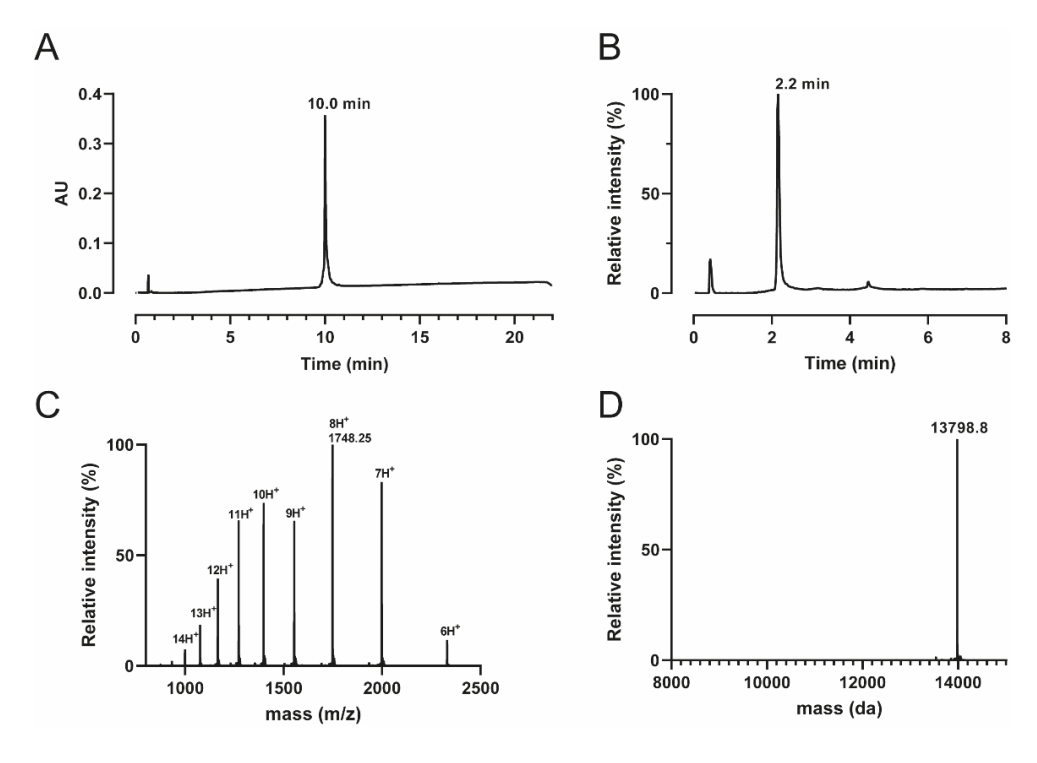
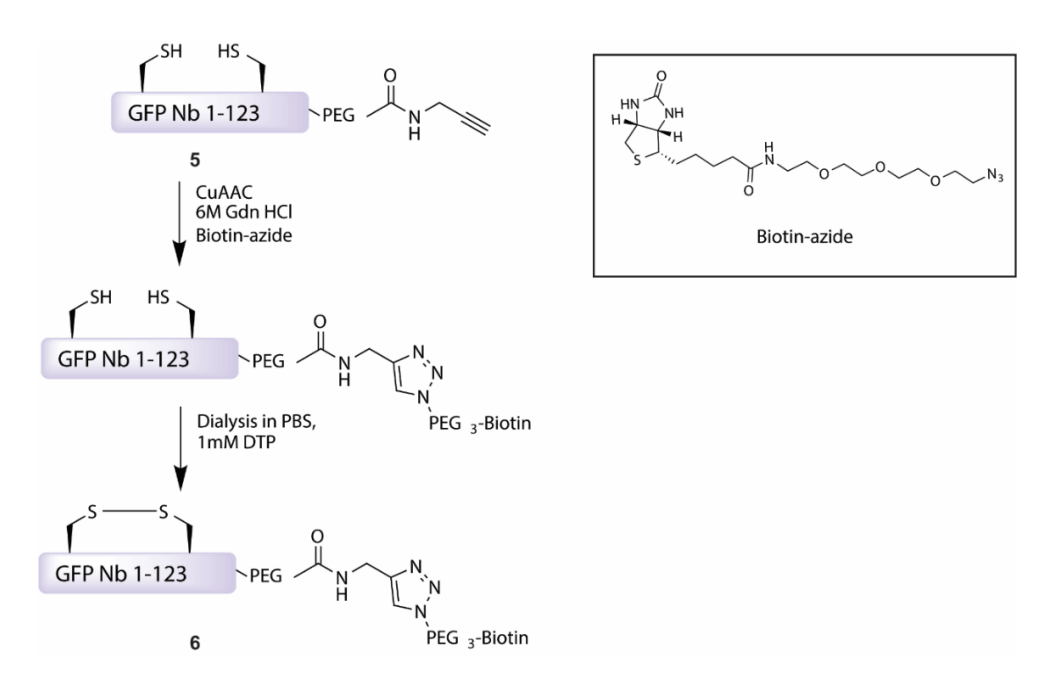


Figure S10. (A) UPLC UV chromatogram (method 1) of folded 5, Rt 10.0 min. (B) Total ion chromatogram (LC-MS method C4) of folded 5, Rt 2.2 min (C) ESI spectrum of folded 5. Calculated Mass (average isotope composition): 13978.4;  $[M+6H]^{6+}$ : 2329.28,  $[M+7H]^{7+}$ : 1996.70,  $[M+8H]^{8+}$ : 1747.21,  $[M+9H]^{9+}$ : 1553.19,  $[M+10H]^{10+}$ : 1398.97,  $[M+11H]^{11+}$ : 1270.97,  $[M+12H]^{12+}$ : 1165.14,  $[M+13H]^{13+}$ : 1075.59,  $[M+14H]^{14+}$ : 998.83. Observed: 13978.8;  $[M+6H]^{6+}$ : 2329.83,  $[M+7H]^{7+}$ : 1997.14,  $[M+8H]^{8+}$ : 1748.25,  $[M+9H]^{9+}$ : 1553.45,  $[M+10H]^{10+}$ : 1398.30,  $[M+11H]^{11+}$ : 1271.18,  $[M+12H]^{12+}$ : 1165.33,  $[M+13H]^{13+}$ : 1075.78,  $[M+14H]^{14+}$ : 999.00. (D) Deconvoluted mass of folded 5, calculated: 13978.4, Observed: 13798.8.

## **CuAAC** chemistry on 5



Scheme S6. Click chemistry on purified 5 followed by disulfide bond formation of 6.

To purified **5** (3.65 mg, 0.26  $\mu$ mol, 1.0 equiv.) in 400  $\mu$ L 6 M Gdn.HCl, 0.2 M phosphate pH 7.2, 25  $\mu$ L of freshly prepared click-mixture (1:1:1  $\nu/\nu/\nu$ , CuSO<sub>4</sub>·5H<sub>2</sub>0 (40.7 mg/mL in water): sodium ascorbate (120 mg/mL in water): THPTA ligand (42.5 mg/mL in water)) was added before adding 65  $\mu$ L of Biotin-PEG-azide (CAS Number: 875770-34-6)(10 mM in DMSO, 0.65  $\mu$ mol, 2.5 equiv.). The reaction was shaken for 60 minutes at room temperature when LC-MS showed full conversion to **6**. The reaction mixture was quenched with 5  $\mu$ L EDTA (0.5 M in MilliQ water) before purification by Äkta, Superdex\* 200 Increase 10/300 GL (flow: 0.5 mL/min) to obtain **6** (2.48 mg, 66 % yield). Thereafter, **6** was folded as previously described for **5**, resulting in folded **6** (Fig S11).

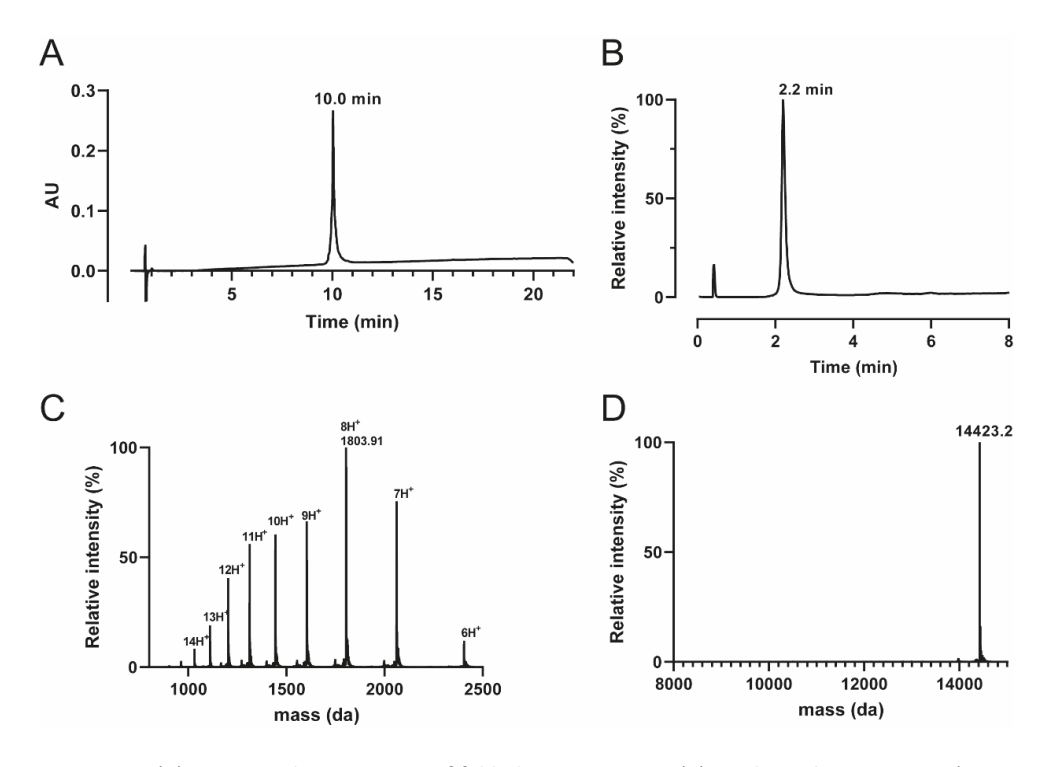
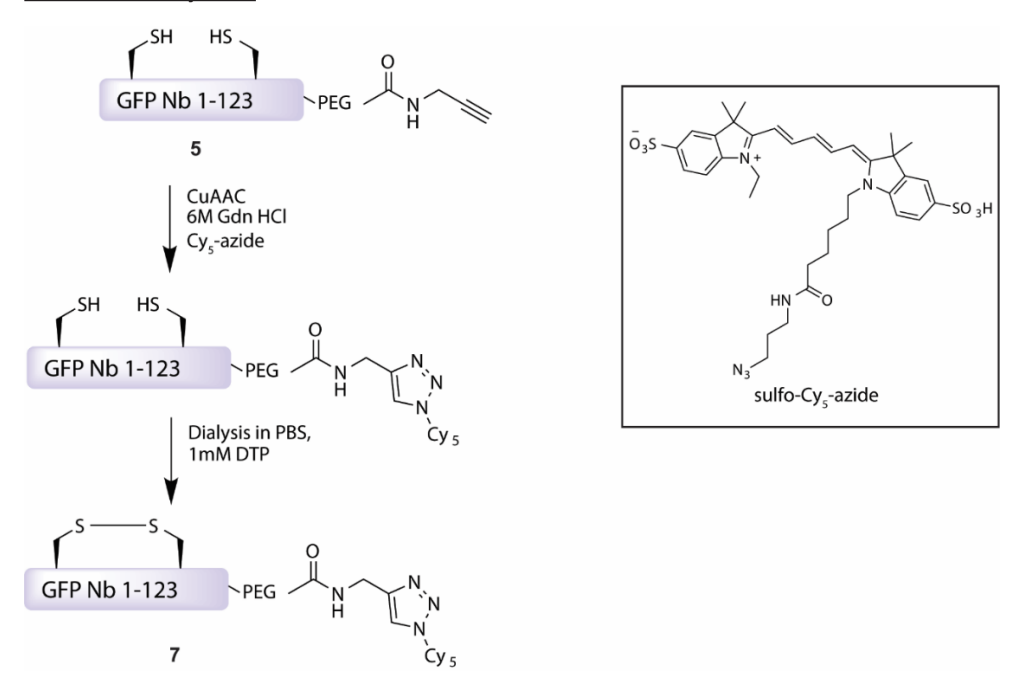


**Figure S11.** (A) UPLC UV chromatogram of folded 6, Rt 10.0 min. (B) Total ion chromatogram (LC-MS method C4) of folded 6, Rt 2.2 min (C) ESI spectrum of folded 6. Calculated Mass (average isotope composition): 14422.9;  $[M+6H]^{6+}$ : 2403.32,  $[M+7H]^{7+}$ : 2060.13,  $[M+8H]^{8+}$ : 1802.74,  $[M+9H]^{9+}$ : 1602.54,  $[M+10H]^{10+}$ : 1442.39,  $[M+11H]^{11+}$ : 1311.35,  $[M+12H]^{12+}$ : 1202.16,  $[M+13H]^{13+}$ : 1109.76,  $[M+14H]^{14+}$ : 1030.56,  $[M+15H]^{15+}$ : 961.93. Observed: Calculated Mass (average isotope composition): 14423.2.4;  $[M+6H]^{6+}$ : 2403.67,  $[M+7H]^{7+}$ : 2060.46,  $[M+8H]^{8+}$ : 1803.16,  $[M+9H]^{9+}$ : 1602.80,  $[M+10H]^{10+}$ : 1442.63,  $[M+11H]^{11+}$ : 1311.56,  $[M+12H]^{12+}$ : 1202.35,  $[M+13H]^{13+}$ : 1109.95,  $[M+14H]^{14+}$ : 1030.73. (D) Deconvoluted mass of folded 6, calculated: 14422.8, observed: 14423.2.

#### Click chemistry on 5



Scheme S7. Click chemistry on purified 5 followed by disulfide bond formation of 7.

To purified **5** (3.65 mg, 0.26  $\mu$ mol, 1.0 equiv.) in 400  $\mu$ L 6 M Gdn.HCl, 0.2 M phosphate pH 7.2, 25  $\mu$ L of freshly prepared click-mixture (1:1:1 v/v/v, CuSO<sub>4</sub>·5H<sub>2</sub>0 (40.7 mg/mL in water): sodium ascorbate (120 mg/mL in water): THPTA ligand (42.5 mg/mL in water)) was added before adding 65  $\mu$ L of sulfo-Cy5-azide (CAS Number. : 1621101-43-6) (10 mM in DMSO, 0.65  $\mu$ mol, 2.5 equiv.). The reaction was shaken for 60 minutes at room temperature when LC-MS showed full conversion of the **7**. The reaction mixture was quenched with 5  $\mu$ L EDTA (0.5M in MilliQ water) before purification by Äkta, Superdex\* 200 Increase 10/300 GL (flow: 0.5 mL/min) to obtain **7** (1.58 mg, 41 % yield). Thereafter, **7** was folded as previously described for **5**, resulting in folded **7** (Fig. S12).

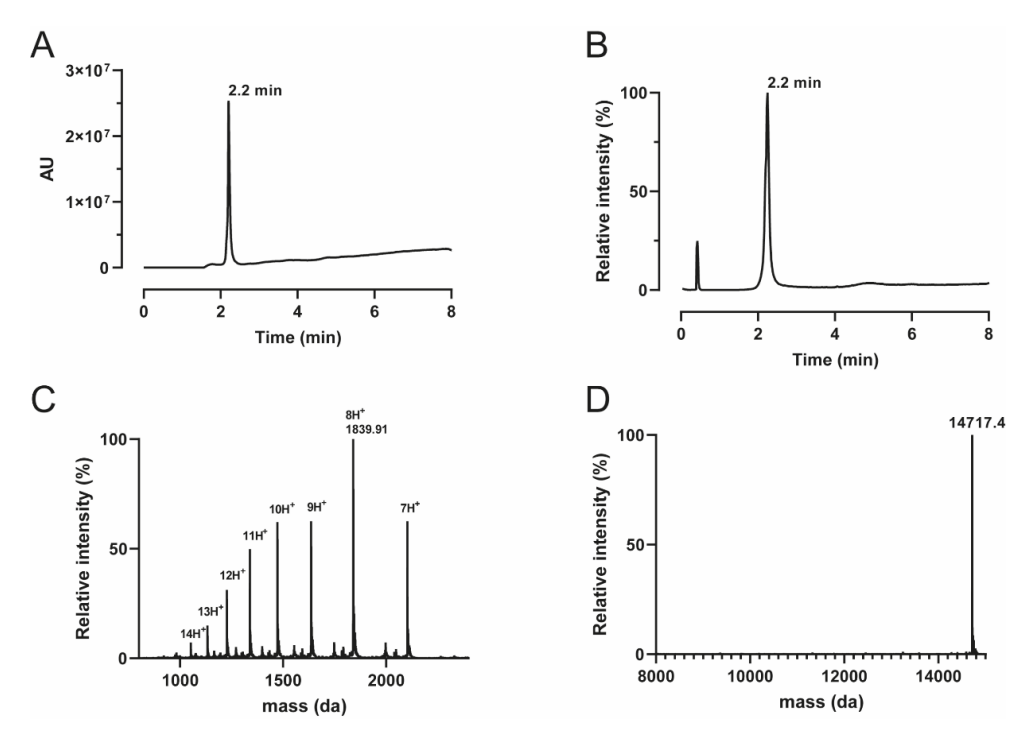


**Figure S12.** (A) UPLC UV chromatogram of folded 7, Rt 10.0 min. (B) Total ion chromatogram (LC-MS method C4) of folded 7, Rt 2.2 min (C) ESI spectrum of folded 7. Calculated Mass (average isotope composition): 14717.3; [M + 6H]<sup>6+</sup>: 2452.33, [M + 7H]<sup>7+</sup>: 2102.14, [M + 8H]<sup>8+</sup>: 1839.50, [M + 9H]<sup>9+</sup>: 1635.22, [M + 10H]<sup>10+</sup>: 1471.80, [M + 11H]<sup>11+</sup>: 1338.09, [M + 12H]<sup>12+</sup>: 1226.66, [M + 13H]<sup>13+</sup>: 1132.38, [M + 14H]<sup>14+</sup>: 1051.56. Observed: Calculated Mass (average isotope composition): 14717.4; [M + 6H]<sup>6+</sup>: 2452.86, [M + 7H]<sup>7+</sup>: 2102.62, [M + 8H]<sup>8+</sup>: 1839.78, [M + 9H]<sup>9+</sup>: 1635.59, [M + 10H]<sup>10+</sup>: 1472.04, [M + 11H]<sup>11+</sup>: 1338.31, [M + 12H]<sup>12+</sup>: 1226.87, [M + 13H]<sup>13+</sup>: 1132.57, [M + 14H]<sup>14+</sup>: 1051.83. (D) Deconvuluted mass of folded 7, calculated: 14717.3 Observed: 14717.4.

#### Circular dichroism

CD measurements were performed using a Jasco 1500 spectropolarimeter at concentrations of 0.1 mg/mL in PBS, pH 7.4, concentrations were measured using a NanoDrop spectrophotometer at A280 (calculated extinction coefficient of 26930 cm<sup>-1</sup>M<sup>-1</sup>). Measurements between 250 and 190 nm were taken using a quartz cuvette with a path length of 0.02 cm. In total, 8 cumulative measurements were made and the average was calculated and plotted using Graphpad PRISM.

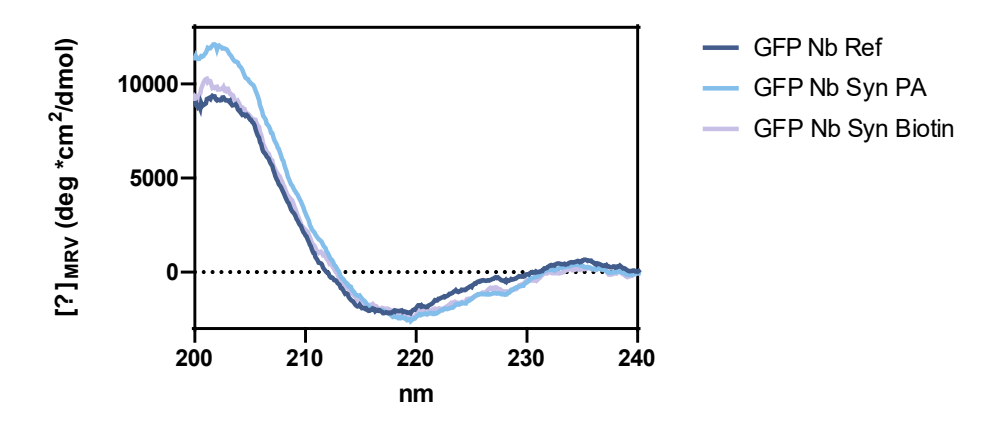


Figure S13. CD chromatogram of the expressed Nb, 5 and 6.

Unfolding CD measurements were performed with a 1 °C/min increase, with a measurement containing 8 scans every 10 °C from 20 °C to 90 °C.

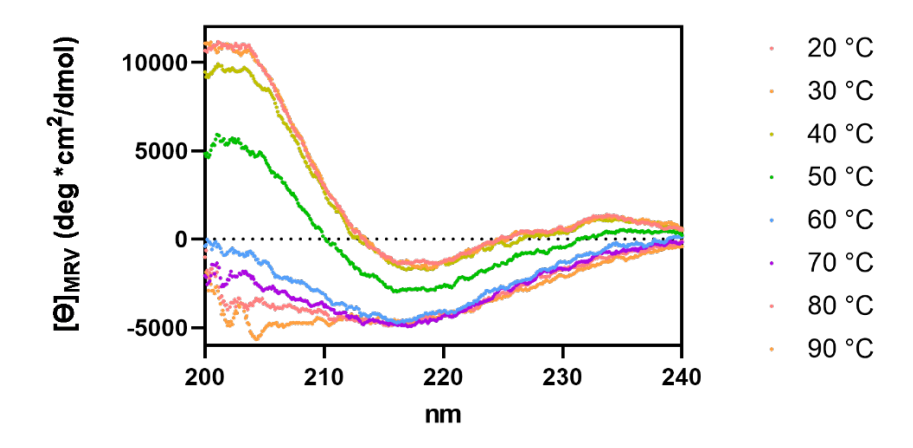


Figure S14. CD spectra of expressed GFP Nb with heating.

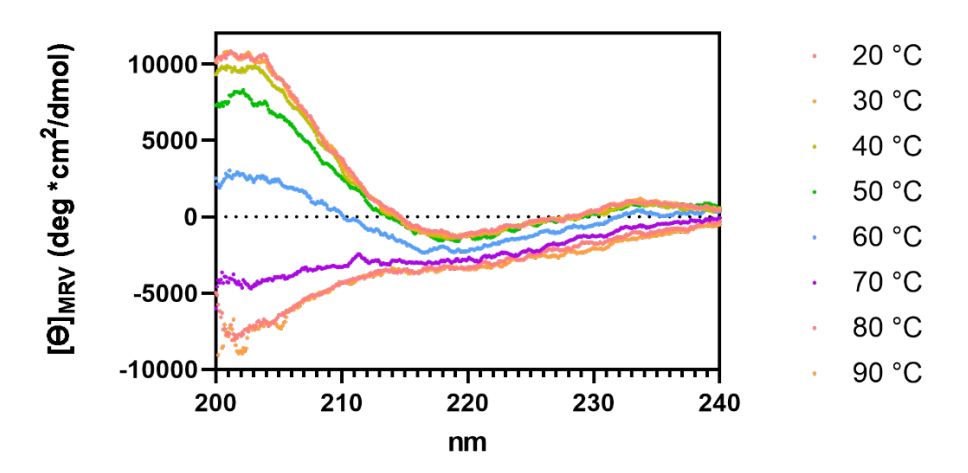


Figure S15. CD spectra of 6 with heating.

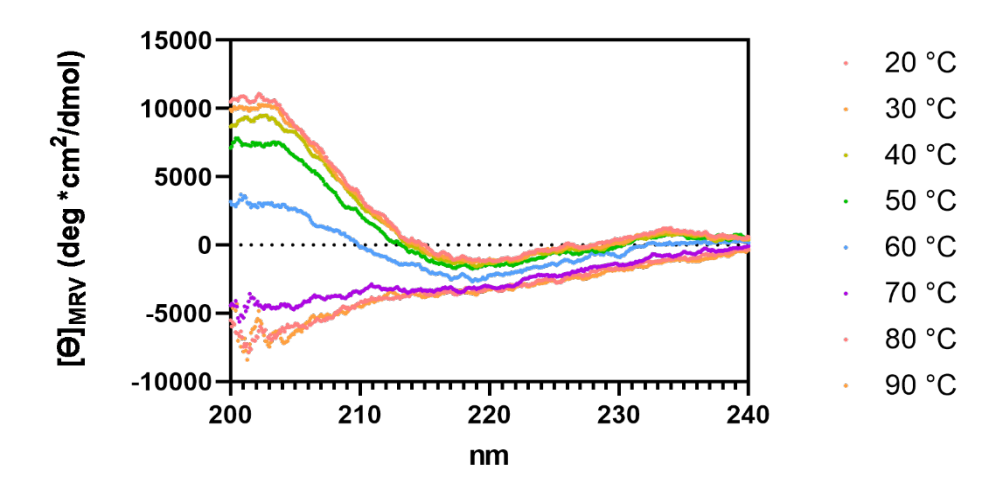


Figure S16. CD spectra of 7 with heating.

## **Bio Layer Interferometry**

Bio Layer Interferometry (BLI) analyses of binding experiments. Graphs show concentrations in nM and fitted curves as dotted lines. The data was fitted using the Octet96 software.

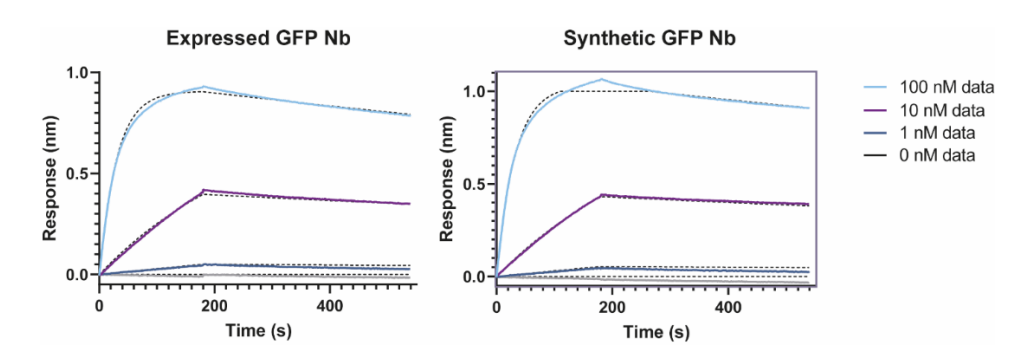


Figure S17. BLI data for binding of the expressed GFP Nb to GFP and the synthetic GFP Nb to GFP.

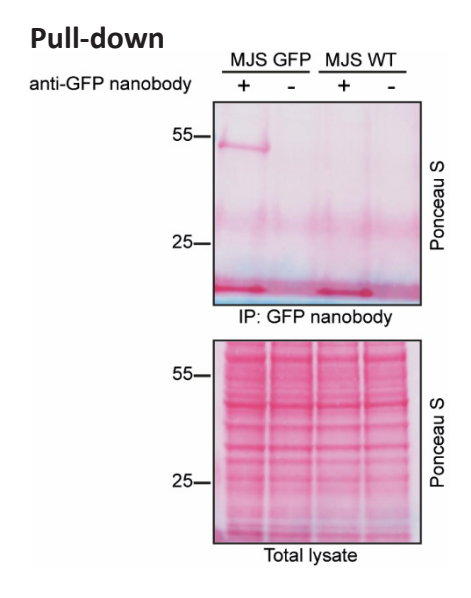


Figure S18. Ponceau S staining of the GFP-Rab7 pull-down. Signal above the 25 kDa marker is streptavidin which is released from the streptavidin beads.

#### References

- 1. Harmsen, M. M. & De Haard, H. J. Properties, production, and applications of cameld single-domain antibody fragments. *Appl Microbiol Biotechnol* **77**, 13–22 (2007).
- 2. Dumoulin, M. *et al.* Single-domain antibody fragments with high conformational stability. *Protein Science* **11**, 500–515 (2009).
- 3. Herce, H. D. *et al.* Cell-permeable nanobodies for targeted immunolabelling and antigen manipulation in living cells. *Nat Chem* **9**, 762–771 (2017).
- 4. Manglik, A., Kobilka, B. K. & Steyaert, J. Nanobodies to Study G Protein-Coupled Receptor Structure and Function. *Annu Rev Pharmacol Toxicol* **57**, 19–37 (2017).
- 5. Cheloha, R. W., Harmand, T. J., Wijne, C., Schwartz, T. U. & Ploegh, H. L. Exploring cellular biochemistry with nanobodies. *Journal of Biological Chemistry* **295**, 15307–15327 (2020).
- 6. Bao, G., Tang, M., Zhao, J. & Zhu, X. Nanobody: a promising toolkit for molecular imaging and disease therapy. *EJNMMI Res* **11**, (2021).
- 7. Wesolowski, J. *et al.* Single domain antibodies: Promising experimental and therapeutic tools in infection and immunity. *Med Microbiol Immunol* **198**, 157–174 (2009).
- 8. Zhang, H. *et al.* Covalently Engineered Nanobody Chimeras for Targeted Membrane Protein Degradation. *J Am Chem Soc* **143**, 16377–16382 (2021).
- 9. Ackaert, C. *et al.* Immunogenicity Risk Profile of Nanobodies. *Front Immunol* **12**, (2021).
- 10. Vincke, C. *et al.* General strategy to humanize a camelid single-domain antibody and identification of a universal humanized nanobody scaffold. *Journal of Biological Chemistry* **284**, 3273–3284 (2009).
- 11. Yang, E. Y. & Shah, K. Nanobodies: Next Generation of Cancer Diagnostics and Therapeutics. *Front Oncol* **10**, (2020).
- Tan, Y., Wu, H., Wei, T. & Li, X. Chemical Protein Synthesis: Advances, Challenges, and Outlooks. *J. Am. Chem. Soc.* 20288–20298 (2020) doi:10.1021/jacs.0c09664.
- 13. Muyldermans, S. Nanobodies: Natural single-domain antibodies. *Annu Rev Biochem* **82**, 775–797 (2013).
- 14. Mitchell, L. S. & Colwell, L. J. Comparative analysis of nanobody sequence and structure data. *Proteins: Structure, Function and Bioinformatics* **86**, 697–706 (2018).
- 15. Kubala, M. H., Kovtun, O., Alexandrov, K. & Collins, B. M. Structural and thermodynamic analysis of the GFP:GFP-nanobody complex. *Protein Science* **19**, 2389–2401 (2010).
- 16. Tornøe, C. W., Christensen, C. & Meldal, M. Peptidotriazoles on solid phase:

- [1,2,3]-Triazoles by regiospecific copper(I)-catalyzed 1,3-dipolar cycloadditions of terminal alkynes to azides. *Journal of Organic Chemistry* **67**, 3057–3064 (2002).
- 17. Paradís-Bas, M., Tulla-Puche, J. & Albericio, F. The road to the synthesis of 'difficult peptides'. *Chem Soc Rev* **45**, 631–654 (2016).
- 18. Hartmann, L. *et al.* VHH characterization. Comparison of recombinant with chemically synthesized anti-HER2 VHH. *Protein Science* **28**, 1865–1879 (2019).
- 19. Fang, G. M. *et al.* Protein chemical synthesis by ligation of peptide hydrazides. *Angewandte Chemie International Edition* **50**, 7645–7649 (2011).
- 20. Kar, A. *et al.* Efficient Chemical Protein Synthesis using Fmoc-Masked N-Terminal Cysteine in Peptide Thioester Segments. *Angewandte Chemie International Edition* **59**, 14796–14801 (2020).
- 21. Giribaldi, J. *et al.* Synthesis, structure and biological activity of CIA and CIB, two  $\alpha$ -conotoxins from the predation-evoked venom of Conus catus. *Toxins (Basel)* **10**, (2018).
- 22. Maruyama, K., Nagasawa, H. & Suzuki, A. 2,2'-Bispyridyl disulfide rapidly induces intramolecular disulfide bonds in peptides. *Peptides (N.Y.)* **20**, 881–884 (1999).
- 23. Sapmaz, A. *et al.* USP32 regulates late endosomal transport and recycling through deubiquitylation of Rab7. *Nat Commun* **10**, 1–18 (2019).
- 24. Guerra, F. & Bucci, C. Multiple roles of the small GTPase Rab7. *Cells* **5**, (2016).
- 25. De Filippis, V., De Antoni, F., Frigo, M., De Laureto, P. P. & Fontana, A. Enhanced protein thermostability by Ala  $\rightarrow$  Aib replacement. *Biochemistry* **37**, 1686–1696 (1998).
- 26. Cabri, W. *et al.* Therapeutic Peptides Targeting PPI in Clinical Development: Overview, Mechanism of Action and Perspectives. *Front Mol Biosci* **8**, 1–21 (2021).
- 27. Rocha, N. *et al.* Cholesterol sensor ORP1L contacts the ER protein VAP to control Rab7-RILP-p150Glued and late endosome positioning. *Journal of Cell Biology* **185**, 1209–1225 (2009).
- 28. Jongsma, M. L. *et al.* SKIP HOPS recruits TBC 1D15 for a Rab7-to-Arl8b identity switch to control late endosome transport . *EMBO J* **39**, 1–25 (2020).
- 29. Cabukusta, B. *et al.* Human VAPome Analysis Reveals MOSPD1 and MOSPD3 as Membrane Contact Site Proteins Interacting with FFAT-Related FFNT Motifs. *Cell Rep* **33**, 108475 (2020).
- 30. Guardia, C. M. *et al.* Reversible association with motor proteins (RAMP): A streptavidin-based method to manipulate organelle positioning. *PLoS Biol* **17**, 1–27 (2019).
- 31. Moorhead, A. M., Jung, J. Y., Smirnov, A., Kaufer, S. & Scidmore, M. A. Multiple host proteins that function in phosphatidylinositol-4-phosphate metabolism are

recruited to the chlamydial inclusion. Infect Immun 78, 1990–2007 (2010).

- 32. Carpino, L. A. *et al.* Synthesis of 'difficult' peptide sequences: application of a depsipeptide technique to the Jung–Redemann 10- and 26-mers and the amyloid peptide A $\beta$ (1–42). *Tetrahedron Lett* **45**, 7519–7523 (2004).
- 33. Mutter, M. *et al.* Switch Peptides In Statu Nascendi: Induction of Conformational Transitions Relevant to Degenerative Diseases. *Angewandte Chemie International Edition* **43**, 4172–4178 (2004).
- 34. Yoshiya, T., Kawashima, H., Sohma, Y., Kimura, T. & Kiso, Y. O-acyl isopeptide method: efficient synthesis of isopeptide segment and application to racemization-free segment condensation. *Org Biomol Chem* **7**, 2894–2904 (2009).